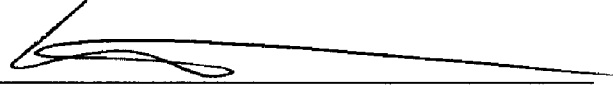


INVESTIGATION OF STRONGLY DUCTED INFRASONIC DISPERSION USING A
VERTICAL EIGENFUNCTION EXPANSION OF THE HELMHOLTZ EQUATION IN
A MODAL BROAD BAND ACOUSTIC PROPAGATION CODE

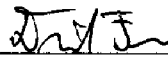
By

Robert Alexander Edon

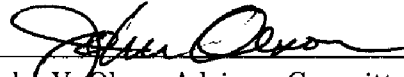
RECOMMENDED:



Dr. Curt A. Szuberla



Dr. David E. Fee



Dr. John V. Olson, Advisory Committee Chair



Dr. Renate A. Wackerbauer, Chair, Department of Physics

INVESTIGATION OF STRONGLY DUCTED INFRASONIC DISPERSION USING A
VERTICAL EIGENFUNCTION EXPANSION OF THE HELMHOLTZ EQUATION IN
A MODAL BROAD BAND ACOUSTIC PROPAGATION CODE

A

PROJECT

Presented to the Faculty

of the University of Alaska Fairbanks

in Partial Fulfillment of the Requirements

for the Degree of

MASTER OF SCIENCE

By

Robert Alexander Edon, B.S.

Fairbanks, Alaska

December 2015

Abstract

This study investigates an infrasound propagation model created by the National Center for Physical Acoustics (NCPA) which is applied to atmospheric data with a strong temperature inversion in the lower atmosphere. This temperature inversion is believed to be the primary cause of a dispersed infrasonic signal recorded by an infrasound sensor array located on the Southern California coast in August, 2012. The received signal is characterized by initial low frequency content followed by a high frequency content tail. It is shown the NCPA model is hindered by limited atmospheric data and no ground truth for the source function which generated the received signal. The results of the NCPA model are shown to not reproduce the recorded signal and provide inconclusive evidence for infrasonic dispersion.

Table of Contents

	Page
Signature Page	i
Title Page	iii
Abstract	v
Table of Contents	vii
List of Figures	ix
List of Tables	xiii
Acknowledgments	xv
Chapter 1 Background and Motivation	1
1.1 Infrasound	1
1.2 Modeling Infrasound Propagation	1
1.3 Observation of Dispersed Signals	2
Chapter 2 Mathematics	5
2.1 Wave Equation	5
2.2 Helmholtz Equation	7
2.3 Dispersion Relations	9
2.4 Vertical Normal Mode Expansion	11
Chapter 3 Methods	13
3.1 Required Files	13
3.2 Atmospheric Data Interpolation	15
Chapter 4 Results	25
4.1 Ray Trace	25
4.2 ModBB	28
Chapter 5 Conclusion	41
References	45
Appendix	47

List of Figures

	Page
1.1 Black Dart signals and spectrogram. The signals shown are two consecutive cannon shots from the USS Dewey. The spectrogram, short-time Fourier Transform of the waveforms, shows the lower frequency content of the signals arrives before the higher frequency content which is an indication of dispersion. . . .	3
1.2 Location of the USS Dewey during Black Dart exercises indicating propagation ranges of interest of 25, 60, and 100 km. Image courtesy of Eric Skowbo.(Skowbo, 2015)	3
2.1 Dispersion relation from the canonical wave equation. Image courtesy of Reijo Rasinkangas.(Reijo Rasinkangas, 2008)	10
3.1 Raw atmospheric data collected during Black Dart exercises.	15
3.2 Atmospheric temperature data collected during Black Dart exercises.	16
3.3 Lower temperature profile. Red points indicate data collected via weather balloon during Black Dart exercises. The green point is the datum collected via ground based instrumentation.	16
3.4 Upper temperature data collected during Black Dart exercises.	17
3.5 Comparison of raw and interpolated data for upper temperature profile. Red and blue points are raw atmospheric data. Blue points are data used to create a curve of best fit. Green points are interpolated data used to smooth out the upper temperature profile and extend it to 40 km.	17
3.6 Difference between raw and interpolated temperature data, $\Delta T = T_{\text{raw}} - T_{\text{interpolated}}$	18
3.7 Interpolated temperature profile.	18
3.8 Atmospheric density data collected during Black Dart exercises.	19
3.9 Lower and upper density data collected during Black Dart exercises.	19
3.10 Lower density profile. Red points indicate data collected via weather balloon during Black Dart exercises. The green points are interpolated data.	20
3.11 Interpolated upper density profile. Red and blue points are raw data. Blue points were used to create a curve of best fit. Green points are interpolated data.	20
3.12 Interpolated density profile.	21
3.13 Atmospheric pressure data collected during Black Dart exercises.	21
3.14 Lower and upper pressure data collected during Black Dart exercises.	22
3.15 Lower pressure profile. Red points indicate data collected via weather balloon during Black Dart exercises. The green point is the interpolated datum.	22
3.16 Interpolated upper pressure profile. Red and blue points are raw data. Blue points were used to create a curve of best fit. Green points are interpolated data.	23
3.17 Interpolated pressure profile.	23

3.18	Interpolated atmospheric data.	24
4.1	Ray trace through a canonical atmosphere.	25
4.2	Effective sound speed of the canonical atmospheric data. Red is c_{eff} as a function of temperature. Blue is c_{eff} as a function of temperature and wind velocity. Black is the speed of sound at the ground.	26
4.3	Ray trace through the Black Dart atmosphere.	27
4.4	Effective sound speed of the Black Dart atmospheric data. Red is c_{eff} as a function of temperature. Black is the speed of sound at the ground.	27
4.5	Ray trace through the Black Dart atmospheric duct.	28
4.6	Initial source pulses used in the ModBB subroutine. Panel 1: the source waveforms. Panel 2: the power spectra of the initial waveforms.	29
4.7	ModBB wave propagation to 100 km with a period of 256 s through the canonical atmosphere.	30
4.8	ModBB wave propagation to 100 km with a period of 512 s through the canonical atmosphere.	31
4.9	ModBB wave propagation to 25 km with a period of 256 s through the Black Dart atmosphere. Panel 1: the propagated waveforms. Panel 2: the power spectra of the propagated waveforms.	32
4.10	ModBB wave propagation to 25 km with a period of 512 s through the Black Dart atmosphere. Panel 1: the propagated waveforms. Panel 2: the power spectra of the propagated waveforms.	32
4.11	ModBB wave propagation to 60 km with a period of 256 s through the Black Dart atmosphere. Panel 1: the propagated waveforms. Panel 2: the power spectra of the propagated waveforms.	33
4.12	ModBB wave propagation to 60 km with a period of 512 s through the Black Dart atmosphere. Panel 1: the propagated waveforms. Panel 2: the power spectra of the propagated waveforms.	34
4.13	ModBB wave propagation to 100 km with a period of 256 s through the Black Dart atmosphere. Panel 1: the propagated waveforms. Panel 2: the power spectra of the propagated waveforms.	35
4.14	ModBB wave propagation to 100 km with a period of 512 s through the Black Dart atmosphere. Panel 1: the propagated waveforms. Panel 2: the power spectra of the propagated waveforms.	35
4.15	Propagated waveform through Black Dart Atmosphere and spectrogram to a range of 25 km with $f_{ textmax} = 0.9$ Hz and T=256 s. Panel 1: propagated waveform through Black Dart atmosphere. Panel 2: spectrogram of the propagated waveform.	37

4.16	Propagated waveform through Black Dart Atmosphere and spectrogram to a range of 60 km with $f_{ textmax} = 2.0$ Hz and $T=256$ s. Panel 1: propagated waveform through Black Dart atmosphere. Panel 2: spectrogram of the propagated waveform.	38
4.17	Propagated waveform through Black Dart Atmosphere and spectrogram to a range of 60 km with $f_{ textmax} = 2.0$ Hz and $T=512$ s. Panel 1: propagated waveform through Black Dart atmosphere. Panel 2: spectrogram of the propagated waveform.	38
4.18	Transmission loss vs. time at a range of 25 km, $f_{max}=0.9$ Hz and $T=256$ s. . .	39

List of Tables

	Page
3.1 Atmospheric data and required units.	13
3.2 Sample of atmospheric data format.	14

Acknowledgments

This work represents one aspect of the effort performed under contracts NSF IIS-0433392 and ONR N00244-11-1-003. These contracts supported work done for the National Consortium for MASINT Research (NCOMR) operated by the National MASINT Office (NMO) of the Defense Intelligence Agency. I would like to recognize the Geophysical Institute (GI) and the Physics Department of the University of Alaska Fairbanks for providing support during the course of this study. Additionally, I would like to thank Eric Skowbo of the Northrop Grumman Corporation for providing data used during this study and Dr. Roger Waxler at the University of Mississippi National Center for Physical Acoustics for providing insight into using the NCPA model.

Chapter 1 Background and Motivation

1.1 Infrasound

Infrasound is the subject of physics which involves the study of sub-audible (low frequency) acoustic pressure waves. That is to say, sound below the threshold of human hearing. Nominally, the infrasound frequency range is between 0.01–20 Hz. Infrasound is not as strongly attenuated in the atmosphere as higher frequency sound, such as audible or ultrasonic waves. Standard acoustic propagation models include a frequency dependent absorption coefficient (see section 2.2.1). The lack of strong attenuation allows infrasonic pressure waves to travel very long distances and provides the opportunity for remote sensing of infrasonic sources in areas where building a sensor array is prohibited by geography, regulation, etc. Waves with frequency content sufficiently larger than the Brunt-Väisälä frequency tend to travel at the same speed, under typical atmospheric conditions, and do not disperse (the frequency content does not spread out in time) as the wave propagates. Coherent signals have been recorded on infrasound arrays tens and even hundreds of kilometers from their source(s).^[1]

The United Nations (UN) governs the Comprehensive Nuclear-Test-Ban Treaty (CTBT) and has created a global network of infrasound and seismic arrays intended to monitor for nuclear explosions. The Wilson Infrasound Observatory (WIO) of the Geophysical Institute (GI), located at the University of Alaska Fairbanks (UAF) and headed by Dr. Curt Szuberla, oversees the operation and maintenance of the infrasound arrays located in United States (U.S.) territory as well as an array located on Antarctica. One such array is located on the UAF campus and is designated IS53.^[4]

1.2 Modeling Infrasound Propagation

Computational modeling of infrasonic propagation is often hindered by assumptions used to determine the governing wave equation. The canonical wave equation uses two fundamental assumptions: the wave behaves adiabatically and the wave pressure is small. The adiabatic approximation is used to describe how energy transfers through the wave and assumes a high frequency limit such that heat does not have sufficient time to flow between areas of compression and rarefaction or between the wave and the environment. The small amplitude of the acoustic pressure assumption allows the wave pressure to be treated as a perturbation on the background pressure which allows the equations governing the conservation of mass and momentum to be truncated to include only linearized terms.

The adiabatic assumption does not properly describe infrasonic waves. The long wavelengths and low frequencies allow ample time for heat to flow between areas of compression and rarefaction. The small wave amplitude assumption is often violated with

explosive or large body sources, such as volcanic eruptions or the oceanic microbarom.^[1,7] A more robust wave equation is developed in section 2.1. Computational methods used to solve more robust wave equations tend to be difficult due to the inclusion of higher order terms and great care must be taken.

This paper investigates an infrasound propagation model created at the National Center for Physical Acoustics (NCPA) located at the University of Mississippi. The NCPA code approaches the numerical computation from a novel mathematical approach (see section 2.4).

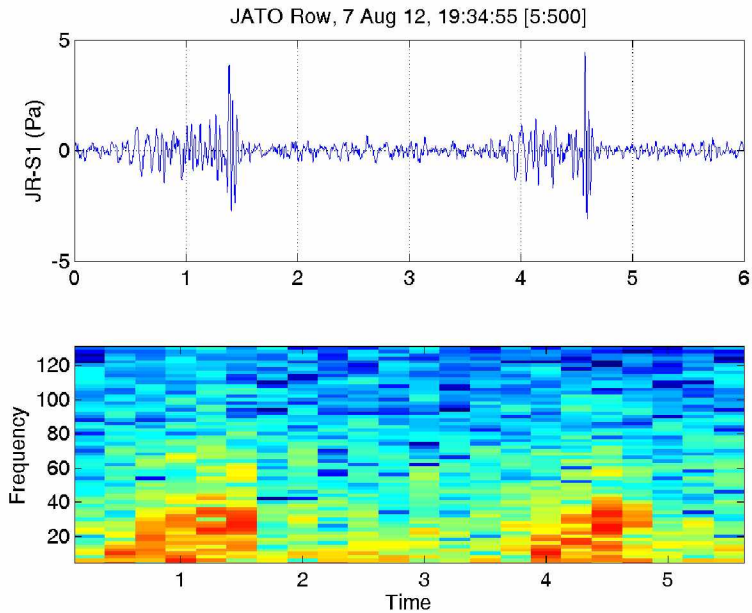
1.3 Observation of Dispersed Signals

In August 2012 Eric Skowbo¹ from Northrop Grumman, in collaboration with Dr. John Olson from UAF, lead a team and deployed a temporary infrasound sensor array at Point Mugu, California. The site designation for this array was dubbed “JATO Row.” The purpose of their study was to record infrasonic signals generated by a series of military exercises being conducted by the U.S. Navy offshore. The name of these particular exercises was Black Dart. Of the various signals collected, one in particular stood out and became the focus of the study presented in this paper. Figure 1.1 shows the recorded signal in panel 1 and its spectrogram in panel 2. The recorded signal is plotted as pressure amplitude (Pa) vs. time (s). The spectrogram is plotted as frequency (Hz) vs. time (s) with the color bins indicating the amplitude of the short-time Fourier transform of the signal. Red \rightarrow blue are the amplitudes from high \rightarrow low of the Fourier transform.

The spectrogram shows the lower frequency content of the signals arrive before the higher frequency content. This seems to indicate the acoustic wave has dispersed during the propagation from the source to the receiver. Information provided by Skowbo indicates the source of this signal was a five inch deck gun aboard the USS Dewey which was located between 25–100 km off the California coast (see Figure 1.2).^[10] This type of gun is believed to produce a standard impulsive, N-wave type source signal.^[2] In such an impulsive source signal the frequency content is packed tightly together, not spread out as seen in Figure 1.1.

Review of the atmospheric data collected during during the Black Dart study show there is a strong temperature inversion near the ground (see Figure 3.1). This lower inversion layer is believed to have created a waveguide which trapped and ducted the acoustic signal near the ground. Such a waveguide has been shown to be characterized by a dispersion relation which is non-linear in frequency and would allow a wave’s frequency content to disperse (spread out in time) even after a short propagation distance (see section 2.3).

¹Northrop Grumman, Program Manager/Lead Systems Engineer for the Research & Technology Division’s Sensors Group, and leads development of the Infrasound Mobile MASINT Unattended Ground Sensor (M2UGS) System.



H

Figure 1.1: Black Dart signals and spectrogram. The signals shown are two consecutive cannon shots from the USS Dewey. The spectrogram, short-time Fourier Transform of the waveforms, shows the lower frequency content of the signals arrives before the higher frequency content which is an indication of dispersion.

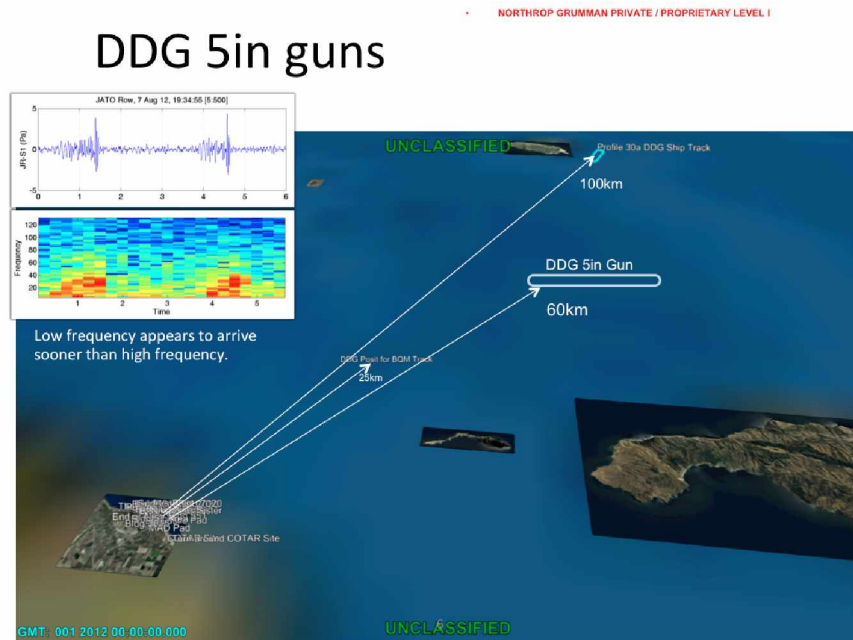


Figure 1.2: Location of the USS Dewey during Black Dart exercises indicating propagation ranges of interest of 25, 60, and 100 km. Image courtesy of Eric Skowbo.^[11]

The purpose of the study presented here is to use the propagation code created by the National Center for Physical Acoustics (hereafter referred to as the NCPA code) to model acoustical propagation through the same atmospheric conditions present during the Black Dart study. Specifically, we are interested in determining if the NCPA code is capable of properly modeling the effects of the waveguide and provide estimates which correlate with the signals recorded in situ.

Chapter 2 Mathematics

2.1 Wave Equation

The equation which governs the propagation of a pressure wave in a homogeneous fluid is known as the wave equation. The simple form is derived from considering the equations of continuity for mass and momentum. The sound speed is given as an effective sound speed and the pressure wave is treated as a perturbation on the background. A thermodynamic assumption is made about the wave propagation process and the continuity equations are then linearized to generate the canonical wave equation (see sections 2.1.2 - 2.1.4).

2.1.1 Effective Sound Speed

The speed of a propagating pressure wave is given as

$$c_{\text{eff}}(z) = c(z) + u(z), \quad (2.1)$$

where $c(z)$ is the velocity of the wave, $u(z)$ is the velocity of the wind component in the direction of the wave, and $c_{\text{eff}}(z)$ is the effective sound speed of the wave in the direction of propagation. A more realistic sound speed model accounts for logarithmic changes due to the wind,^[9] but the NCPA model utilizes the more simple approximation given by Eq. (2.1).

2.1.2 Continuity Equations

The equation for the conservation of mass is

$$\frac{\partial \rho_a}{\partial t} + \nabla \cdot (\rho_a \vec{v}_a) = 0, \quad (2.2)$$

where ρ_a and \vec{v}_a are the density and velocity of the atmosphere, respectively (the subscript “a” indicates atmosphere). The $\partial \rho_a / \partial t$ term represents the time rate of change in the density of a small parcel or volume of air, and the $\nabla \cdot (\rho_a \vec{v}_a)$ represents the spatial flow of fluid through the parcel.

The equation for the conservation of momentum is

$$\rho_a \frac{D\vec{v}_a}{Dt} = -\nabla p_a, \quad (2.3)$$

where p_a is the atmospheric pressure and $D/Dt \equiv \partial/\partial t + \vec{v}_a \cdot \nabla$ is the time derivative in the reference frame of the locally moving fluid.

2.1.3 Perturbations on the Background

The signal pressure (p), density (ρ), and velocity (\vec{v}) are treated as perturbations on the background values which are average values in a region of the atmosphere (p_{av} , ρ_{av} , \vec{v}_{av}). The atmospheric pressure (p_a), density (ρ_a), and velocity (\vec{v}_a) are then written as

$$\begin{aligned}
p_{\mathbf{a}} &= p_{\text{av}} + p \\
\rho_{\mathbf{a}} &= \rho_{\text{av}} + \rho \\
\vec{v}_{\mathbf{a}} &= \vec{v}_{\text{av}} + \vec{v}.
\end{aligned}
\tag{2.4}$$

The canonical wave equation now makes two assumptions: 1) the atmosphere is homogeneous (i.e. non-layered) and 2) there is no wind (i.e. $\vec{v}_{\text{av}} = 0$).

2.1.4 Linearization of Continuity Equations

Inserting Eqns. (2.4) into Eqns. (2.2) and (2.3) and keeping only the linear terms yields

$$\rho_{\text{av}} \nabla \cdot \vec{v} = -\frac{\partial \rho}{\partial t} \tag{2.5}$$

$$\rho_{\text{av}} \frac{\partial \vec{v}}{\partial t} = -\nabla p. \tag{2.6}$$

These two equations are known as the linear acoustic equations.^[9]

2.1.5 Adiabatic Process Assumption

The form of the thermodynamic process is based on the assumption that the sound wave fluctuations are rapid. If the fluctuations are rapid enough the system will not transfer heat or mass. This allows us to assume the process is adiabatic and therefore the pressure and density follow the relation

$$p_{\mathbf{a}} = K \rho_{\mathbf{a}}^{\gamma}, \tag{2.7}$$

where K is a constant and γ is the ratio of specific heats ($\gamma = c_p/c_v$). Expanding Eq. (2.7) to the first-order using a Taylor expansion of $p_{\mathbf{a}}(\rho_{\mathbf{a}})$ gives

$$p_{\mathbf{a}}(\rho_{\text{av}} + \rho) = p_{\text{av}} + \left(\frac{\partial p_{\mathbf{a}}}{\partial \rho_{\mathbf{a}}} \right)_{\text{av}} \rho. \tag{2.8}$$

Using the first of Eqns. (2.4) ($p = p_{\mathbf{a}} - p_{\text{av}}$) and Eq. (2.7) we find

$$p = c^2 \rho, \tag{2.9}$$

where

$$c^2 \equiv \left(\frac{\partial p_{\mathbf{a}}}{\partial \rho_{\mathbf{a}}} \right)_{\text{av}} = \gamma \frac{p_{\text{av}}}{\rho_{\text{av}}}. \tag{2.10}$$

Assuming the atmosphere is an ideal-gas we can find the quantity c^2 in a more useful

form. The ideal-gas law, written in terms of density, is

$$p_{\text{av}} = \rho_{\text{av}}RT, \quad (2.11)$$

where R is the ideal-gas constant and T is the absolute temperature. Inserting Eq. (2.11) into Eq. (2.10) gives

$$c^2 = \gamma RT. \quad (2.12)$$

With the adiabatic assumption we may substitute Eq. (2.9) into Eqns. (2.5) and (2.6) and write them as

$$\rho \nabla \cdot \vec{v} = -\frac{1}{c^2} \frac{\partial p}{\partial t} \quad (2.13)$$

$$\rho \frac{\partial \vec{v}}{\partial t} = -\nabla p. \quad (2.14)$$

The subscripts have been removed for simplicity since all terms are average quantities. Taking the time derivative of Eq. (2.13) and the divergence of Eq. (2.14) we may remove the $\partial(\nabla \cdot \vec{v})/\partial t$ term and arrive at the canonical wave equation:

$$\nabla^2 p - \frac{1}{c^2} \frac{\partial^2 p}{\partial t^2} = 0. \quad (2.15)$$

The assumptions required to derive this equation yield a simple approximation of a propagating wave in the atmosphere. However, real atmospheres have wind and are stratified. Infrasound is characterized by low frequency, long wavelength sound waves and the adiabatic assumption does not hold.

The NCPA code uses a more realistic wave equation which accounts for a stratified atmosphere as well as wind and is known as the Helmholtz equation.

2.2 Helmholtz Equation

2.2.1 Perturbations on the Background

To account for the stratified, windy atmosphere we augment Eqns. (2.4) to account for a vertical (z) dependence as well as x-, y-, and z-components of the wind vector (u , v , and w , respectively). The acoustic wave is still treated as a perturbation on the background and is now represented by

$$\begin{aligned}
p_{\mathbf{a}} &= p_{\text{av}}(z) + p \\
\rho_{\mathbf{a}} &= \rho_{\text{av}}(z) + \rho \\
\vec{v}_{\mathbf{a}} &= (u_{\text{av}} + u, v_{\text{av}} + v, w).
\end{aligned}
\tag{2.16}$$

Assuming the pressure wave is harmonic in nature (i.e. pressure and velocity have a simple $e^{i\omega t}$ dependence) allows us to them as

$$\begin{aligned}
p &= \Re(p_c e^{i\omega t}) \\
\vec{v} &= \Re(\vec{v}_c e^{i\omega t}),
\end{aligned}
\tag{2.17}$$

where p_c and \vec{v}_c are complex amplitudes.^[9] This harmonic assumption reduces the linear acoustic equations, Eqns. (2.5) and (2.6), to forms where the time derivative becomes a factor of $i\omega$:

$$\begin{aligned}
\rho c^2 \nabla \cdot \vec{v}_c &= i\omega p_c \\
i\omega \rho \vec{v}_c &= \nabla p_c.
\end{aligned}
\tag{2.18}$$

The canonical wave equation, Eq. (2.15), reduces to

$$\nabla^2 p_c + k^2 p_c = 0.
\tag{2.19}$$

Equation (2.19) is known as the Helmholtz equation and applies to windy, stratified atmospheres for harmonic sound waves. Limiting our study to point sources we may approach this equation using Green's theorem for a fluid half space and arrive at the Helmholtz equation in two dimensions written in cylindrical coordinates:^[5]

$$\frac{1}{r} \frac{\partial}{\partial r} \left(r \frac{\partial p}{\partial r} \right) + \rho(z) \frac{\partial}{\partial z} \left(\frac{1}{\rho(z)} \frac{\partial p}{\partial z} \right) + \frac{\omega^2}{c^2(z)} p = -\frac{\delta(r) \delta(z - z_s)}{2\pi r},
\tag{2.20}$$

where r is the radial distance from the source, p is the pressure, $\rho(z)$ is the altitude dependent atmospheric density, $\omega = 2\pi f = kc$ is the angular frequency of the wave, and $c(z)$ is the altitude dependent effective wave speed. The motivation for using cylindrical coordinates comes from the geometry of propagation. As the wave moves away from the source it spreads spherically in space. Since the atmospheric data only contains a vertical dependence there is symmetry in the horizontal angle. It is therefore convenient to choose a coordinate system where only the distance from the source, r , and height, z , are independent variables.

This two dimensional variant of the Helmholtz equation is the underlying equa-

tion solved by the NCPA code for a point source located at $\delta(r)\delta(z - z_s)$. The effective sound speed accounts for atmospheric absorption and damping by including an imaginary component:

$$c(z) = c_0(z) + \vec{v}_0(z) \cdot \hat{k}_r + ia(\omega), \quad (2.21)$$

where $c_0(z)$ is the original sound speed, $\vec{v}_0(z) \cdot \hat{k}_r$ is the component of the wind velocity in the radial direction of propagation, and $a(\omega)$ is a frequency dependent absorption coefficient.

2.3 Dispersion Relations

Generally speaking, any equation which relates the wave number k to the angular frequency ω may be regarded as a dispersion relation. From the canonical wave equation the dispersion equation can be shown to be written as^[3]

$$k_z^2 = (\omega_b^2 - \omega^2) \frac{k_x^2}{\omega^2} - \frac{(\omega_a^2 - \omega^2)}{c^2}, \quad (2.22)$$

where k_z is the vertical component of the wave number, k_x is the horizontal component of the wave number, ω is the angular frequency of the wave, c is the wave speed, and ω_a and ω_b are the acoustic cutoff frequency and Brunt-Väisälä frequency given by

$$\omega_a^2 = \frac{\gamma^2 g^2}{4c^2} \quad (2.23)$$

$$\omega_b^2 = (\gamma - 1) \frac{g^2}{c^2}, \quad (2.24)$$

where γ is the ratio of specific heats, and g is gravitational acceleration. This form of the dispersion relation can be shown to yield a constant group velocity (ω/k) for sufficiently large frequencies. Very low frequencies, approaching the Brunt-Väisälä frequency, however, are slower. The Brunt-Väisälä frequency itself has zero group velocity (i.e. $\omega/k = 0$).

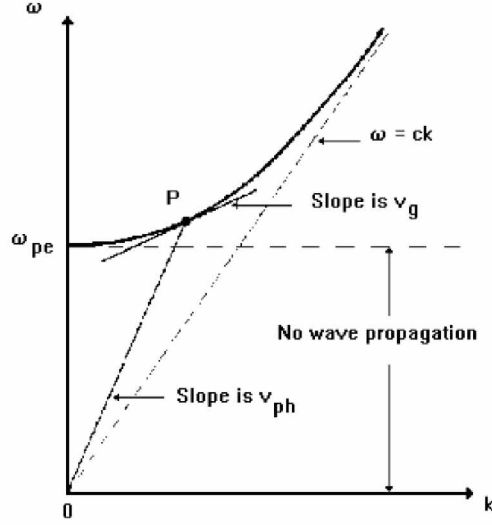


Figure 2.1: Dispersion relation from the canonical wave equation. Image courtesy of Reijo Rasinkangas.^[8]

Another means of deriving a dispersion relation may be done by purely geometrical means. Assuming a uniform waveguide characterized by a single air density ρ wedged between a rigid ground and a rigid half space with air density ρ' , it can be shown the dispersion relation is^[6]

$$kH\sqrt{\frac{c^2}{\alpha^2} - 1} - \arctan \frac{\rho}{\rho'} \sqrt{\frac{\frac{\alpha^2}{c^2} - \frac{c^2}{\alpha'^2}}{1 - \frac{\alpha^2}{c^2}}} = n\pi, \quad (2.25)$$

where ρ is the atmospheric density in the waveguide, ρ' is the atmospheric density in the half space above the waveguide, α is the sound velocity for waves trapped in the waveguide, c is the sound speed for propagation parallel to the ground, and H is the height of the waveguide. Despite the rudimentary approach of this method, the dispersion relation is clearly non-linear (i.e. each frequency will travel at a different group velocity within the waveguide).

The large temperature inversion seen in the Black Dart atmospheric data (Figure 3.1) strongly refracts acoustic waves towards the ground. The atmosphere above the inversion may act similarly to a rigid fluid half space and a dispersion relation similar to the one shown in Eq. (2.25) may be applicable. The simple analysis of Negraru and Herrin^[6] does not model real atmospheres but it does lend evidence to the large temperature inversion seen in the Black Dart data being a potential cause of the received dispersed signal at JATO Row.

2.4 Vertical Normal Mode Expansion

Waveguides created from a strong inversion layer in the lower atmosphere have been found to exist in a number of situations, such as the nocturnal boundary layer.^[13] At the core of the NCPA code is the methodology of Waxler et. al. wherein they use a normal mode expansion of the vertical eigenfunctions to explore the long range propagation of impulsive infrasonic sources under strongly ducted nocturnal conditions.^[12,13,15,16] Other work in the field of propagation has made use of the parabolic equation or horizontal wave number integration techniques. These approaches are computationally intensive and fail to provide a physical motivation for the dynamics behind the acoustic propagation.^[12]

Each of the normal modes propagating in a waveguide must satisfy the the Helmholtz equation, Eq. (2.19), as well as the following boundary condition at the ground:

$$\left. \frac{\partial p}{\partial z} \right|_{z=0} = -C(\omega)p, \quad (2.26)$$

where $C(\omega)$ is related the ground impedance $Z(\omega)$ by

$$Z(\omega) = \frac{i\omega\rho_0(0)}{C(\omega)}. \quad (2.27)$$

Applying separation of variables to the Helmholtz equation for the vertical component gives

$$\left(\frac{d^2}{dz^2} + k(z)^2 - \eta \right) \psi(z) = 0, \quad (2.28)$$

where η is the separation parameter or eigenvalue. Applying a WKB approximation to Eq. (2.28) yields solutions with an asymptotic form^[13]

$$\psi(z) \approx (k(z)^2 - \eta)^{-1/4} \left(A e^{i \int_{z_0}^z \sqrt{k(z')^2 - \eta} dz'} + B e^{-i \int_{z_0}^z \sqrt{k(z')^2 - \eta} dz'} \right). \quad (2.29)$$

Assuming η is purely real these solutions are oscillatory and do not satisfy the upper atmosphere boundary condition (the amplitude of sound waves should tend towards zero at the atmosphere becomes thinner). If $\Im \eta \neq 0$ the solutions of Eq. (2.28) in the WKB approximation have two general forms: those which exponentially increase and those which exponentially decrease with increasing altitude, z . The solutions which exponentially decrease satisfy the upper atmosphere boundary condition and have an asymptotic form^[13]

$$\psi(z) \approx A \begin{cases} (k(z)^2 - \eta)^{-1/4} e^{i \int_{z_0}^z \sqrt{k(z')^2 - \eta} dz'} & \text{if } \Im \eta > 0 \\ (k(z)^2 - \eta)^{-1/4} e^{-i \int_{z_0}^z \sqrt{k(z')^2 - \eta} dz'} & \text{if } \Im \eta < 0. \end{cases}$$

These solutions do not, in general, satisfy the boundary condition at the ground, Eq. (2.26). However, certain values of η do satisfy both boundary conditions. This discrete

set of values is referred to by Waxler as the point spectrum.

Solving for the eigenvalues, η , which satisfy the boundary conditions is not trivial and requires a two-dimensional parameter search in a complex plane. Such searches are numerically unstable due to the exponential growth of the functions being searched. However, Waxler develops subtle computational tricks which help maintain the stability of the code and prevent the solutions from diverging towards infinity.^[13] Once the eigenvalues η are known they are used in Eq. (2.28) subject to the boundary condition at the ground, Eq. (2.26), and numerically solved by standard forward differencing or center differencing schemes. Thus the NCPA code is capable of propagating an infrasonic pressure wave through an atmosphere while avoiding common divergent solutions found when using simpler approaches.

Chapter 3 Methods

This chapter discusses the necessary steps required to run the NCPA code (section 3.1) as well as the modifications to the collected atmospheric data used in this study (section 3.2).

3.1 Required Files

To implement the NCPA code two input files are required: 1) an atmospheric data file (section 3.1.1) and 2) a “.options” file which specifies the parameters to be used (section 3.1.2).

3.1.1 Atmospheric Data File

The atmospheric data file is an ASCII code data file containing the recorded data from the area around or between the source and the receiver. The required data is the altitude above sea level (z), x -, y -, and z -components of the wind vector (u , v , w), temperature (t), air density (d), and air pressure (p). These parameters may be specified in any order, given at the command line or in the “.options” file, but will be used and referred to in the standard order of $zuvwtdp$. The required units for the atmospheric data are given in Table 3.1.

Table 3.1: Atmospheric data and required units.

Atmospheric Parameter	NCPA Parameter	NCPA Unit Required
Altitude	z	km
Wind velocity (all components)	u, v, w	m/s
Air temperature	t	K
Air density	d	g/cm^3
Air pressure	p	hPa

The NCPA code also requires the values of the atmospheric data to be presented in a standardized format using scientific notation. Data collected using weather balloon, radiosonde, satellite, etc. will likely not match the required units and Matlab, or a similar program, will be needed to correct this. The atmospheric data used in this study was collected via weather balloon and the units were modified using Matlab. A sample of the ASCII file is depicted in Table 3.2 which shows the proper formatting to be used with the NCPA code.

Table 3.2: Sample of atmospheric data format.

z	u	v	w	t	d	p
0.0000000e+00	0.0000000e+00	0.0000000e+00	0.0000000e+00	2.9560000e+02	1.1893000e-03	5.1960000e+01
1.40210003-02	0.0000000e+00	0.0000000e+00	0.0000000e+00	2.9475000e+02	1.1893000e-03	1.0138000e+03
3.0480000e-02	0.0000000e+00	0.0000000e+00	0.0000000e+00	2.9115000e-03	1.2021000e-03	1.0118000e+03
⋮	⋮	⋮	⋮	⋮	⋮	⋮

The first line of Table 3.2 (“zuvwtdp”) is displayed for demonstration purposes only and is not required. If the data file does contain such a line of text the NCPA code will fail to properly read the data unless the line is skipped at the command line or using the “.options” file.

3.1.2 The “.options” File

The “.options” file is a text file containing the various options to be used when the NCPA code executes. An example file name used in this study is “ModBB_00_7_60_256_bd.options.” The naming scheme was designed to quickly determine several key parameters contained within the file. In this scheme the NCPA subroutine used, maximum frequency, range, period, and atmospheric data file are indicated. The contents of this file are shown below:

```

../bin/ModBB --out_disp_src2rcv_file dispersionfile.dat --atmosfile \
Black_Dart_Data_File_Corrected_No_Wind_Interpolated2.dat \
--atmosfileorder zuvwdp --skiplines 0 --azimuth 90 \
--f_step 0.00390625 --f_max 0.7 --use_modess

../bin/ModBB --pulse_prop_src2rcv dispersionfile.dat --range_R_km 60 \
--waveform_out_file output_waveform.dat --use_builtin_pulse

```

The “.options” file reduces the amount of typing at the command line by embedding the same commands in an easily accessible text file. A more detailed description of the required and optional parameters needed to run the ModBB subroutine may be found in Appendix A.

During the course of this study the ModBB subroutine was used to propagate a pulse built into the code to ranges of 25, 60, and 100 km using periods of 256 and 512 s. Maximum frequencies investigated were between 0.5 and 2.0 Hz. While the actual signal investigated during this study contains frequencies up to about 30–40 Hz, the computational power of the computers used limited the investigation to lower frequencies. Additionally,

the output results from the ModBB subroutine became suspect for frequencies above 2 Hz.

3.2 Atmospheric Data Interpolation

The raw atmospheric data (Figure 3.1) contains 242 points each for the altitude (z), x , y , and z -components of the wind (u , v , and w , respectively), temperature (t), density (d), and pressure (p). The altitude range is ≈ 0.014 – 19.96 km. This needed to be extended to the ground as well as to a maximum of about 40 km to allow the NCPA code to properly calculate the eigenfunction solutions for a propagating wave.^[14] To achieve this, artificial data were added to the altitude and the temperature, density, and pressure data were interpolated to the new atmospheric limits. Additionally, some smoothing of the temperature profile was done.

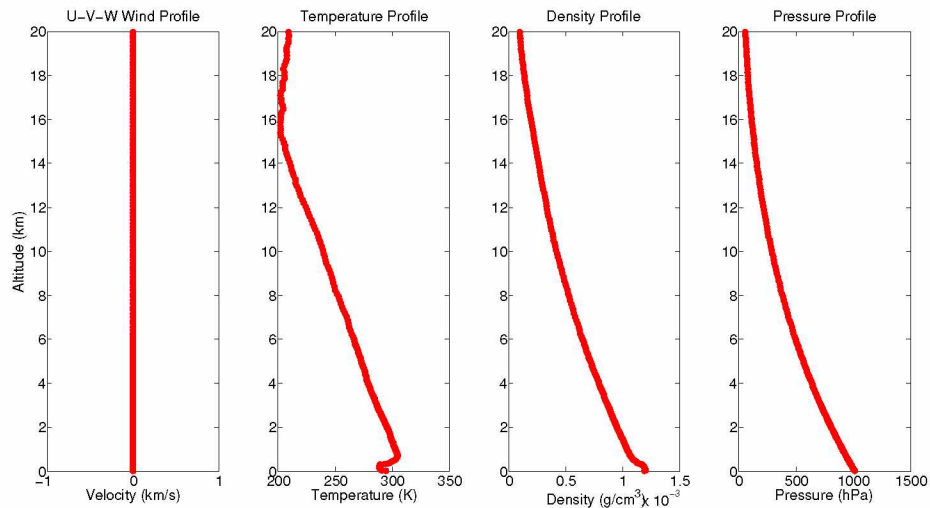


Figure 3.1: Raw atmospheric data collected during Black Dart exercises.

3.2.1 Altitude Expansion

The atmospheric data file included with the NCPA sample files (referred to from hereon as the canonical data) contained canonical sample atmospheric profiles ranging from 0–200 km with 0.1 km spacing between each point. This spacing was preserved as well as possible when extending the raw atmospheric data. Due to the lowest altitude being about 14 m above the ground only a single artificial point was added to the lower profile (at 0 km). In correspondence with Roger Waxler it was suggested to extend the atmosphere up to about 40 km so the NCPA code could properly compute the propagation of a pressure wave.^[14] An additional 201 artificial data points were added to the upper profile of the raw data giving a total of 444 altitude points ranging from 0–40.064 km.

3.2.2 Temperature Interpolation

The temperature data collected during the Black Dart exercises is shown in Figure 3.2.

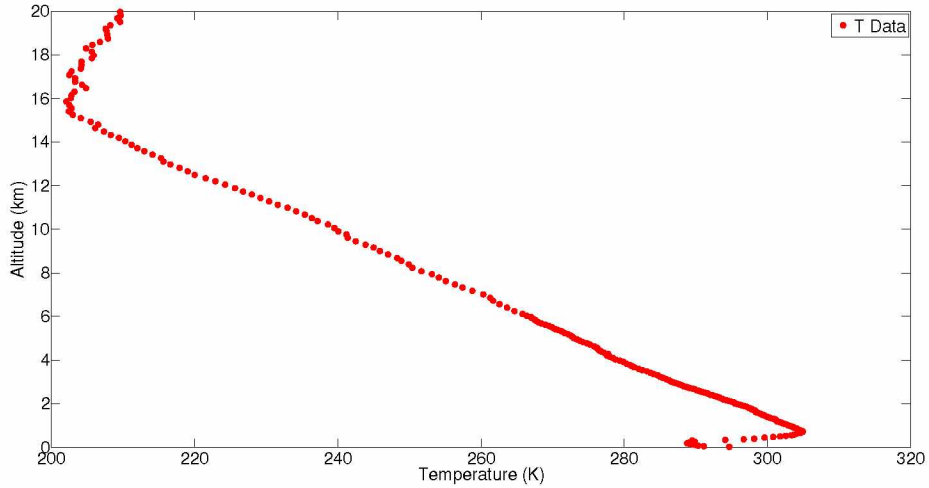


Figure 3.2: Atmospheric temperature data collected during Black Dart exercises.

The temperature profile was extended to the ground using data collected at the infrasonic array site JATO Row via ground based weather instrumentation.^[11] The new lower temperature profile with Skowbo's ground data included is shown in Figure 3.3. The red points are the data collected via weather balloon and the green point is the datum collected via ground based instrumentation by Skowbo.

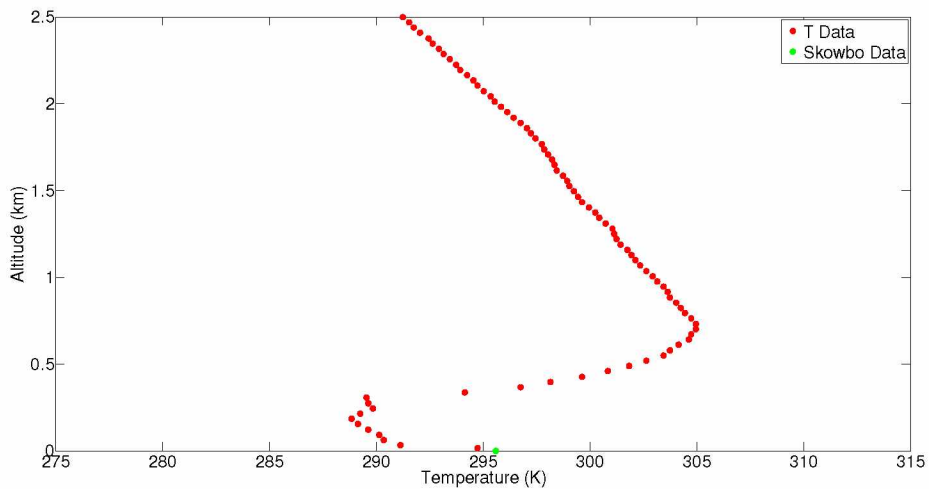


Figure 3.3: Lower temperature profile. Red points indicate data collected via weather balloon during Black Dart exercises. The green point is the datum collected via ground based instrumentation.

The upper temperature profile (Figure 3.4) has some erratic behavior which was

smoothed as well as extended to 40 km. The general shape of the upper inversion appears to be quadratic in altitude and so this type of function was chosen for the interpolation.

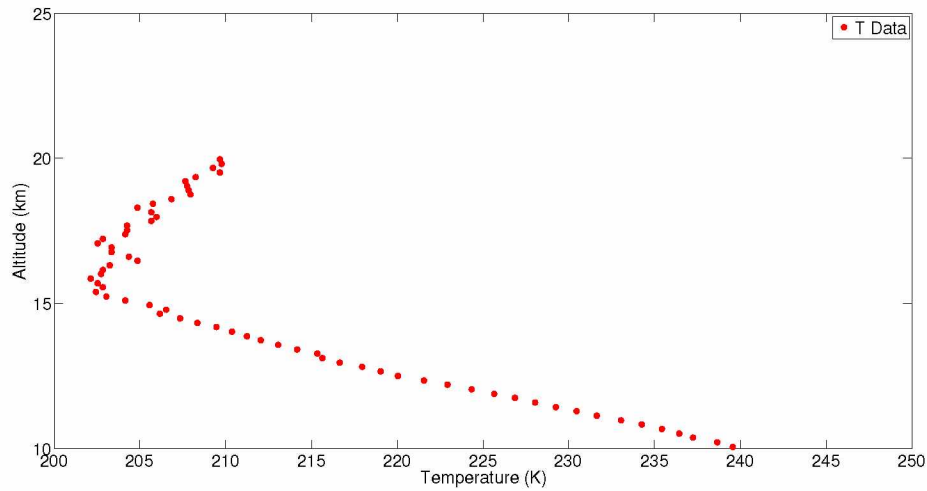


Figure 3.4: Upper temperature data collected during Black Dart exercises.

Panel 1 of Figure 3.5 shows the raw temperature data in red and blue. The blue points were used to create a curve of best fit. The green points are interpolated data to be added to the upper temperature profile. Panel 2 of Figure 3.5 shows the new upper temperature profile with raw data in red and interpolated data in green.

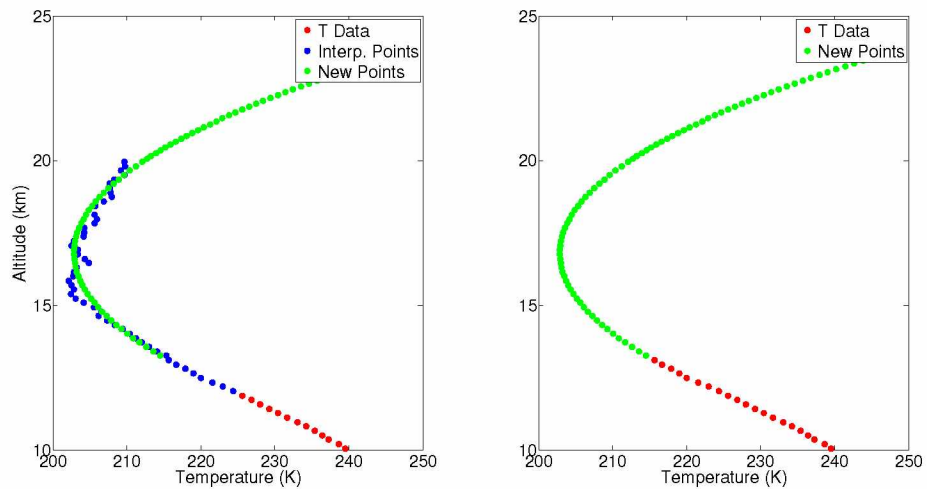


Figure 3.5: Comparison of raw and interpolated data for upper temperature profile. Red and blue points are raw atmospheric data. Blue points are data used to create a curve of best fit. Green points are interpolated data used to smooth out the upper temperature profile and extend it to 40 km.

To justify replacing the raw temperature data with the interpolated points we compare the difference between the two. Figure 3.6 shows $\Delta T = T_{\text{raw}} - T_{\text{interpolated}}$.

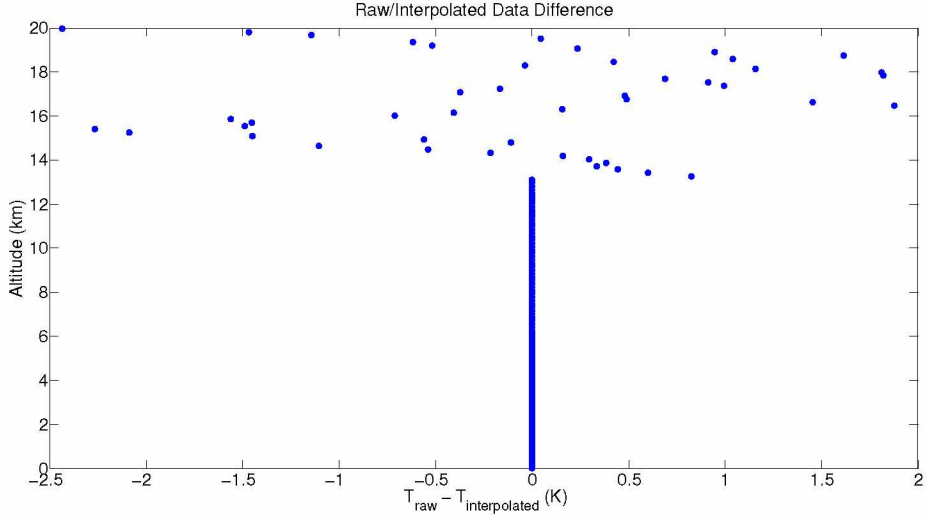


Figure 3.6: Difference between raw and interpolated temperature data, $\Delta T = T_{\text{raw}} - T_{\text{interpolated}}$.

The absolute maximum difference between the raw and interpolated temperature data is 2.44 K with a mean absolute difference of 0.17 K. The temperature values in the upper inversion layer are $\approx 200\text{--}215$ K which give an absolute maximum percentage difference of 1.14–1.22% and a mean absolute percentage difference of 0.08–0.09%. The difference is small enough to justify replacing the raw data. The smooth upper temperature profile is believed to make the NCPA code subroutines run more efficiently and provide a more accurate model for a propagated wave.

The final interpolated temperature profile to be used in the NCPA code is shown in Figure 3.7.

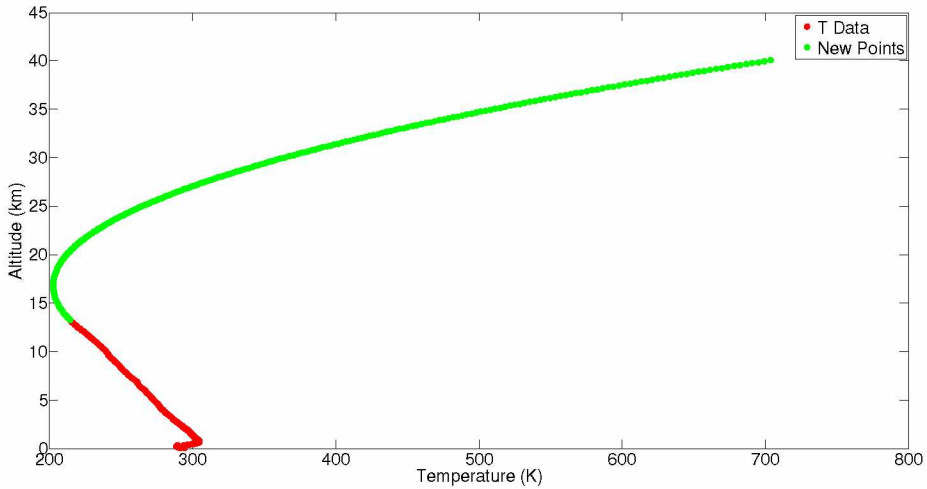


Figure 3.7: Interpolated temperature profile.

3.2.3 Density Interpolation

The raw density data collected during the Black Dart exercises is shown in Figure 3.8.

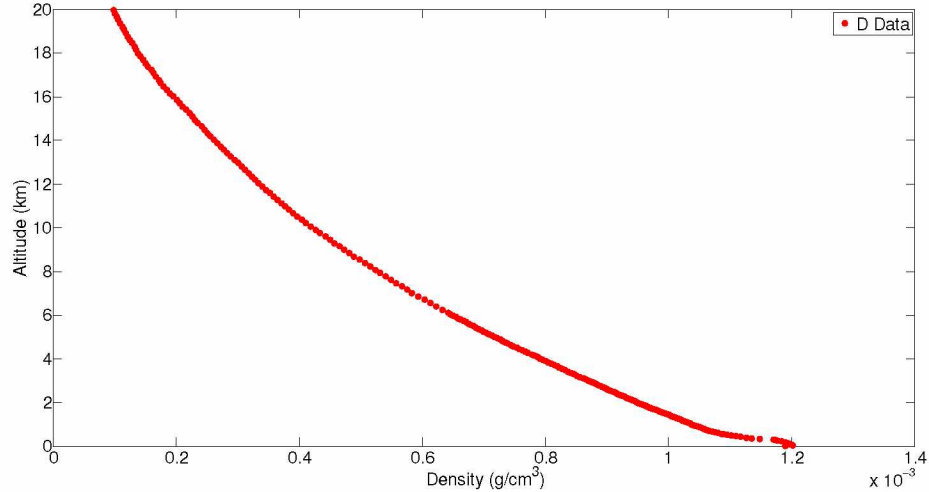


Figure 3.8: Atmospheric density data collected during Black Dart exercises.

Panel 1 of Figure 3.9 shows the lower density profile and panel 2 shows the upper density profile.

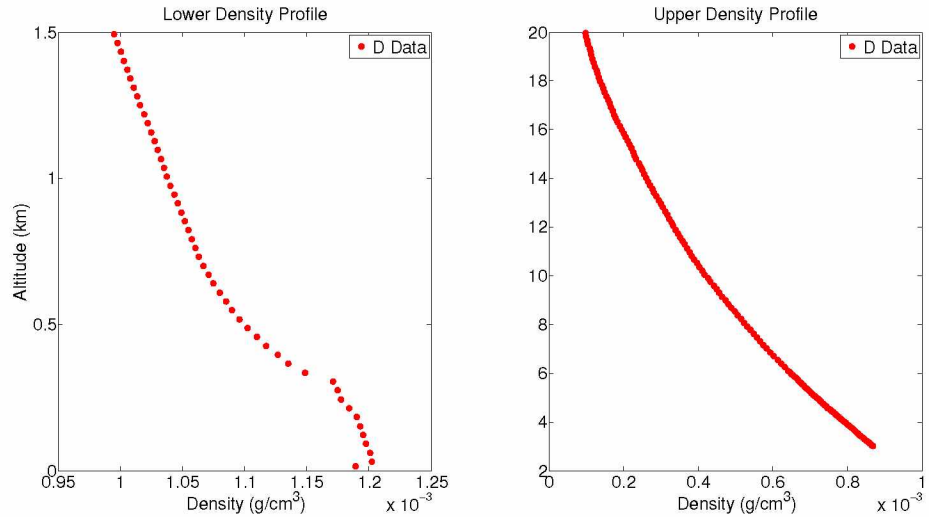


Figure 3.9: Lower and upper density data collected during Black Dart exercises.

The lower density profile has a linear trend near the ground. However, the lowest data point does not match this trend. A linear interpolation was used to extend the density data to the ground and the outlying point was replaced. Figure 3.10 shows the new lower density profile. The raw data is plotted in red and the interpolated data is green.

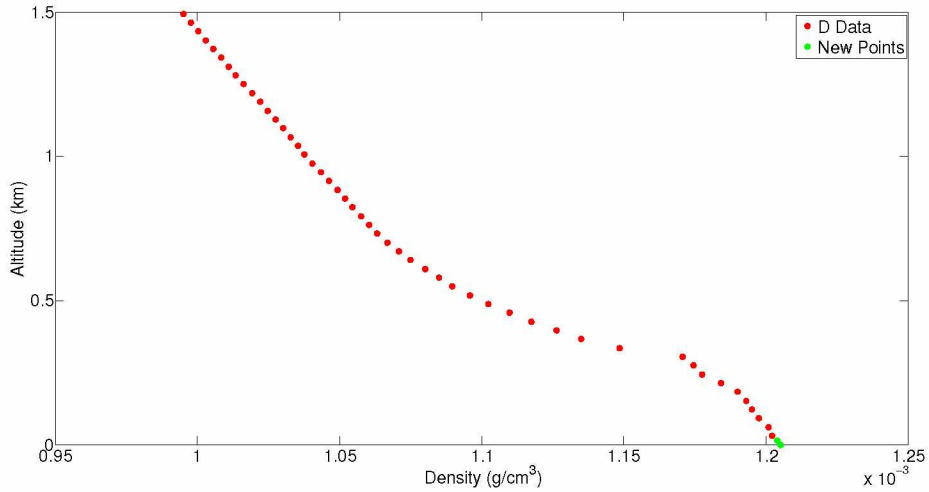


Figure 3.10: Lower density profile. Red points indicate data collected via weather balloon during Black Dart exercises. The green points are interpolated data.

The upper density profile appears to follow an exponential trend. Figure 3.11 shows the raw density data in red and blue. The blue points were used to create a curve of best fit and interpolate the density to 40 km. The green points are the interpolated data.

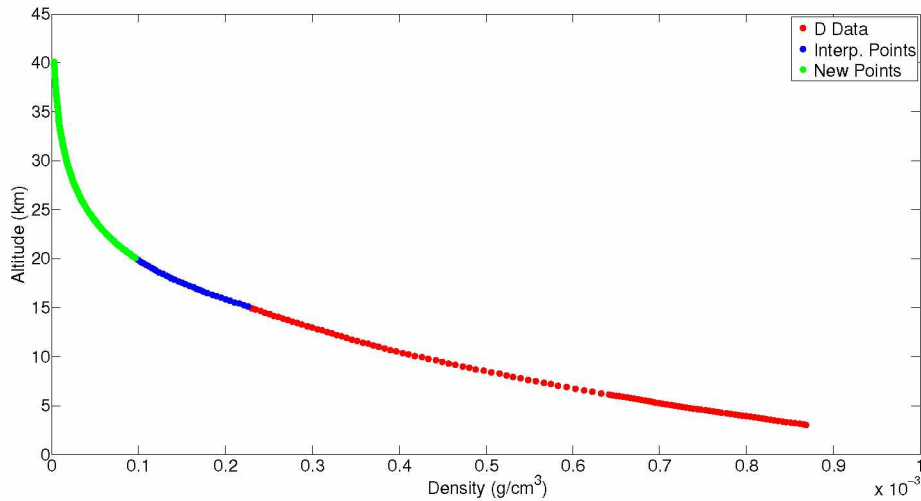


Figure 3.11: Interpolated upper density profile. Red and blue points are raw data. Blue points were used to create a curve of best fit. Green points are interpolated data.

The final interpolated density profile to be used in the NCPA code is shown in Figure 3.12.

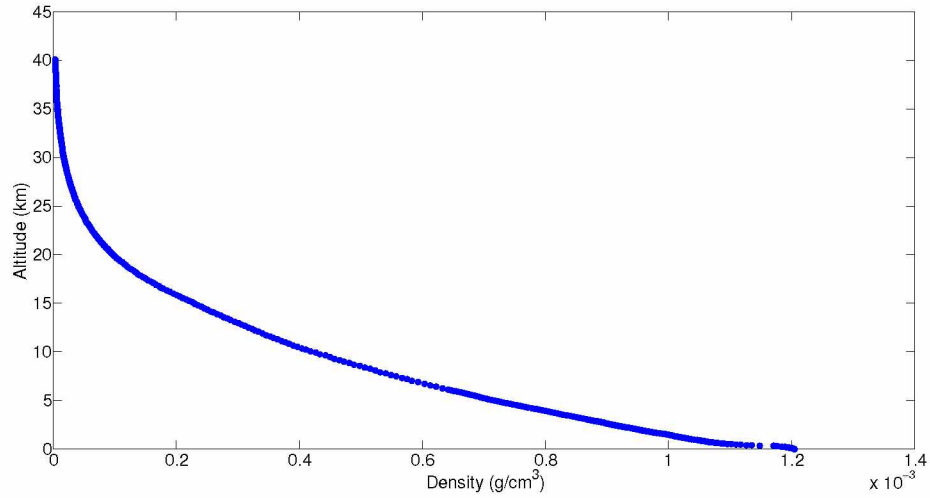


Figure 3.12: Interpolated density profile.

3.2.4 Pressure Interpolation

The pressure data collected during the Black Dart exercises is shown in Figure 3.13.

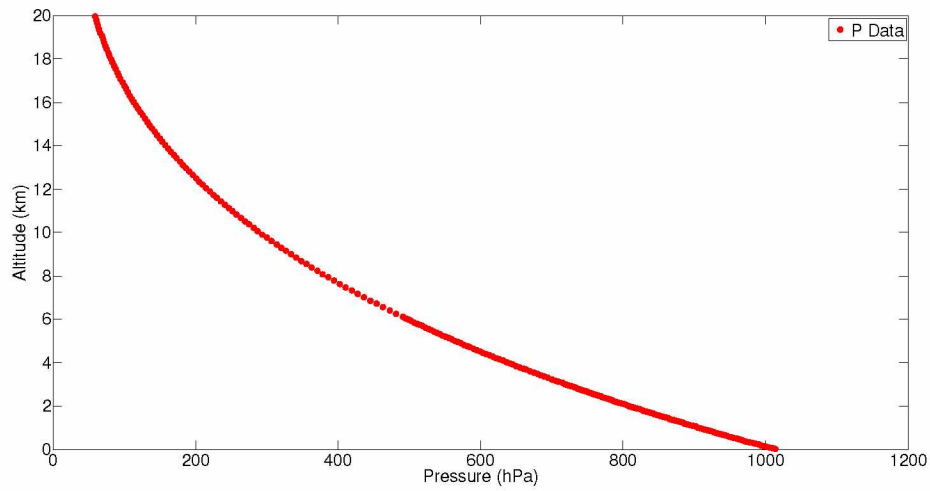


Figure 3.13: Atmospheric pressure data collected during Black Dart exercises.

Panel 1 of Figure 3.14 shows the lower pressure profile and panel 2 shows the upper pressure profile.

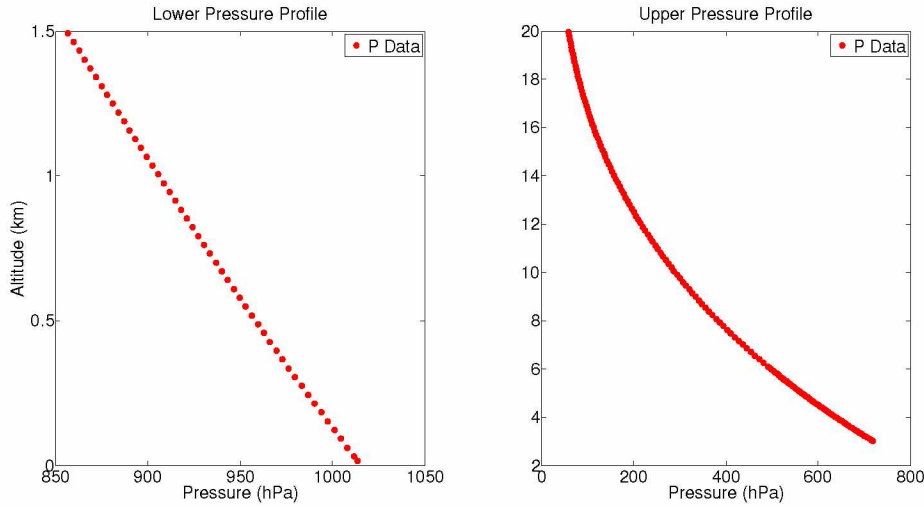


Figure 3.14: Lower and upper pressure data collected during Black Dart exercises.

The lower pressure profile has a linear trend near the ground and a linear interpolation was used to extend it to the ground. Figure 3.15 shows the new lower pressure profile. The raw data is plotted in red and the interpolated data is green.

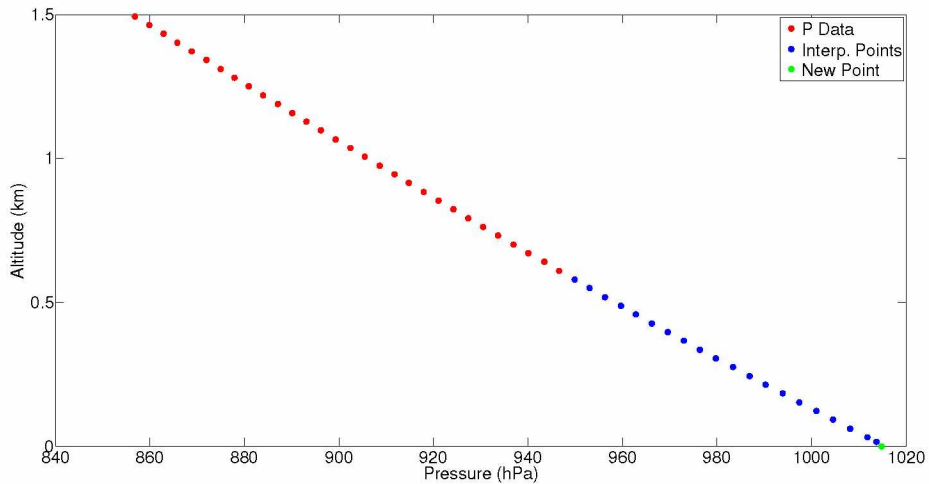


Figure 3.15: Lower pressure profile. Red points indicate data collected via weather balloon during Black Dart exercises. The green point is the interpolated datum.

The upper pressure profile appears to follow an exponential trend. Figure 3.16 shows the raw pressure data in red and blue. The blue points were used to create a curve of best fit and interpolate the pressure to 40 km. The green points are the interpolated data.

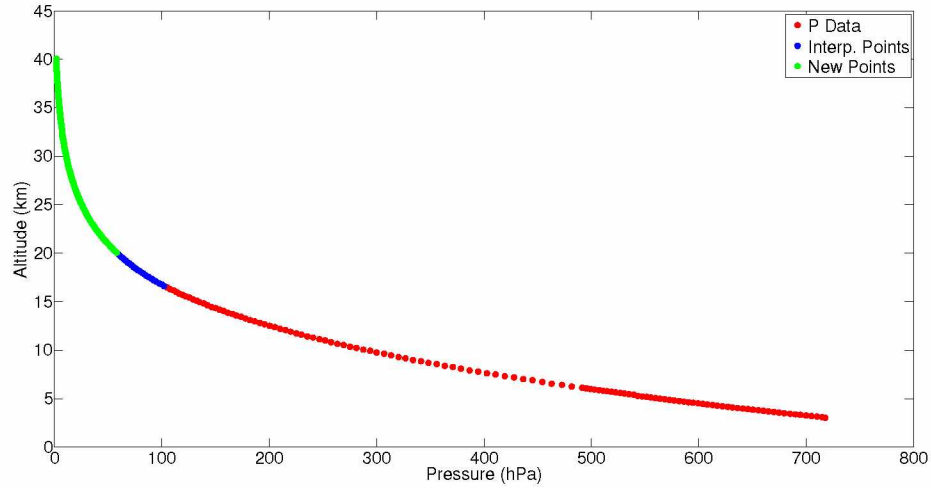


Figure 3.16: Interpolated upper pressure profile. Red and blue points are raw data. Blue points were used to create a curve of best fit. Green points are interpolated data.

The final interpolated pressure profile to be used in the NCPA code is shown in Figure 3.17.

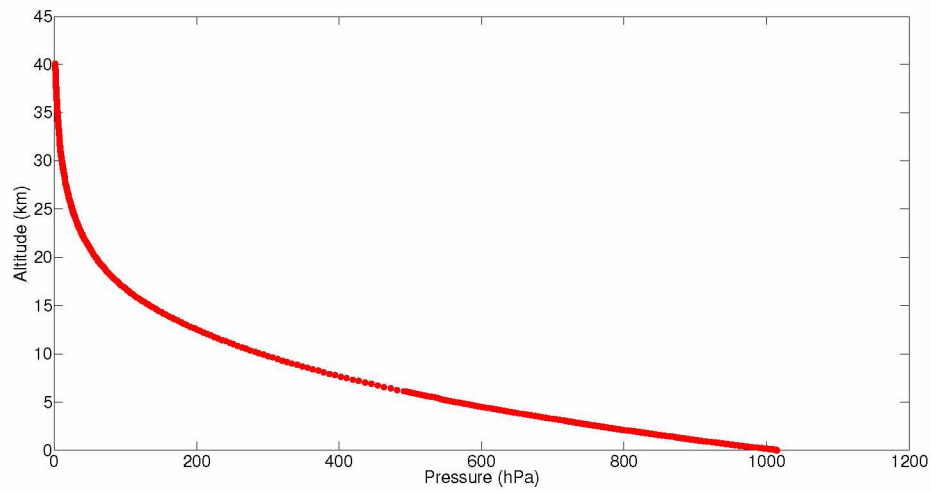


Figure 3.17: Interpolated pressure profile.

3.2.5 Interpolated Atmospheric Data

The new interpolated atmospheric data are shown in Figure 3.18

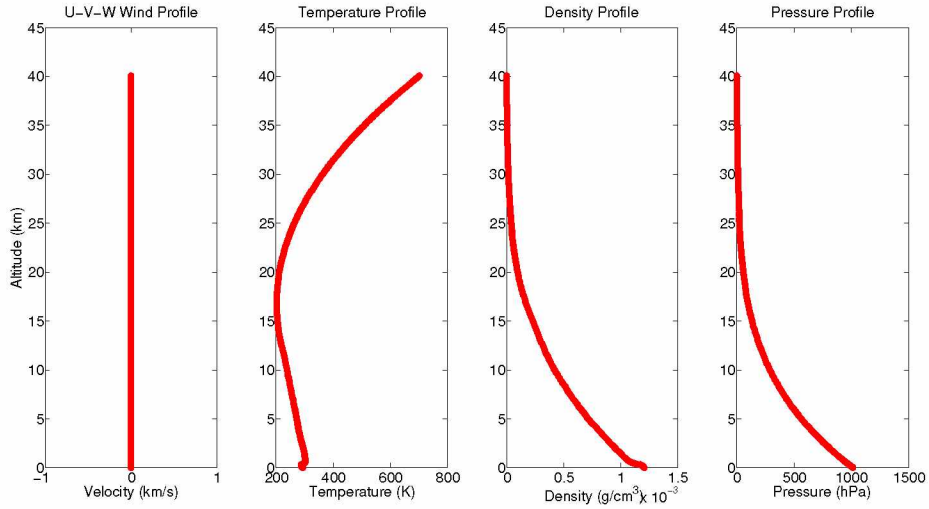


Figure 3.18: Interpolated atmospheric data.

The wind data was collected using a unit which was never determined. As such it was decided to zero out the wind data as shown in panel 1 of Figure 3.18 for this study. This will create differences in the output waveforms of the NCPA code but is not believed to greatly alter any dispersion effects due to the lower temperature inversion.

Chapter 4 Results

This chapter presents the results of the ray trace (section 4.1) and ModBB (section 4.2) as applied to this study. The ModBB subroutine is a Modal Broad Band propagation code developed based on the the work of Waxler et. al. (see section 2.4).^[12,13,15,16]

4.1 Ray Trace

Ray traces provide a useful estimate as a first approximation in wave propagation. Its use is limited as it assumes a frequency independent approach to the propagation as well as a simple layered atmosphere. Most ray trace programs solve Snell's Law of refraction based on the temperature at a certain altitude. Despite this limitation, it will be shown the atmospheric data collected during the Black Dart exercises does create a ducting waveguide in the lower atmosphere.

The NCPA ray trace subroutine was used as a baseline comparison between the canonical atmosphere (section 4.1.1) and the Black Dart atmosphere (section 4.1.2). Further, it was used to determine the period to be used in the ModBB subroutine and provide some justification for the three chosen propagation ranges of 25, 60, and 100 km.

4.1.1 Canonical Atmosphere

Figure 4.1 shows the results of the ray trace subroutine through the toy atmosphere for propagation out to 110 km and propagation angles between 0–20°, measured from the surface horizontal. The rays do not show strong arrival clusters due to the even spread along the ground. Furthermore, the results are atypical of a standard atmosphere.

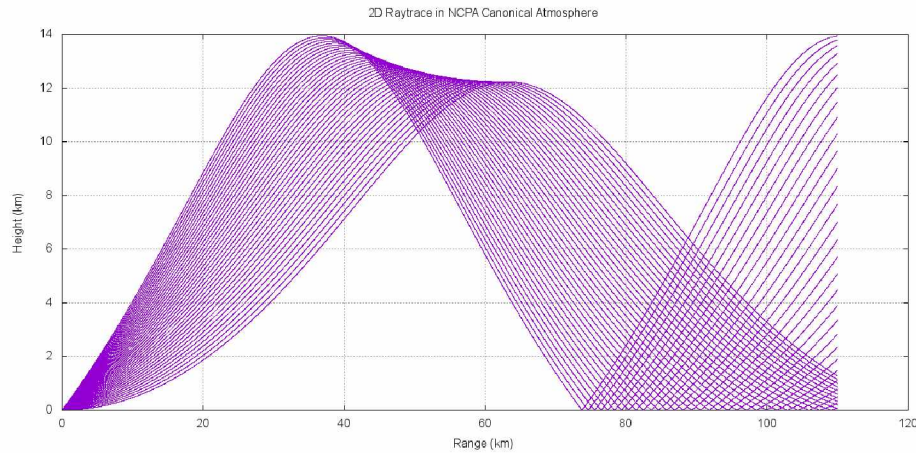


Figure 4.1: Ray trace through a canonical atmosphere.

These atypical results do not seem to be physical. Investigation of the canonical atmospheric data indicates the temperature and wind profiles should cause rays to refract

towards the ground around an altitude above 40 km. Figure 4.2 shows the effective sound speed, c_{eff} , as a function of temperature and wind velocity for the canonical atmospheric data.

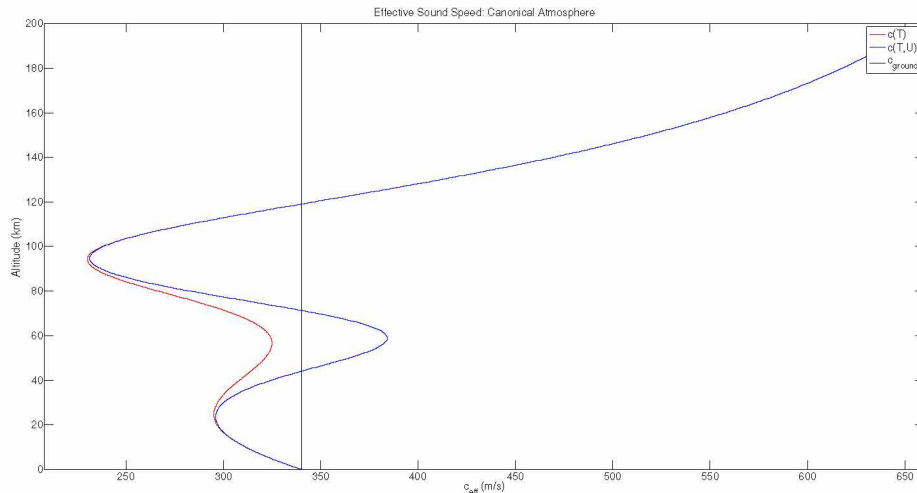


Figure 4.2: Effective sound speed of the canonical atmospheric data. Red is c_{eff} as a function of temperature. Blue is c_{eff} as a function of temperature and wind velocity. Black is the speed of sound at the ground.

In general, the effective sound speed needs to be larger than the speed of sound at the ground before an acoustic signal will refract back down towards the ground. Figure 4.2 clearly indicates this should occur at an altitude above 40 km. It is currently unknown why the ray trace results using the canonical atmosphere predict downward refracting rays at altitudes between 10–14 km.

4.1.2 Black Dart Atmosphere

Figure 4.3 shows the results of the ray trace subroutine using the Black Dart atmosphere and the same propagation range and launch angles as specified in section 4.1.1. Rays emitted at angles greater than 10.2° from the ground travel upwards similar to those in the toy atmosphere. These rays do not return to the ground within the propagation range of interest or do not show strong arrival clusters at the ground. As such, they are unlikely to affect the rays propagating in the duct and are excluded from this study. Rays emitted below 10.2° are clearly ducted by the strong lower inversion at ≈ 1 km.

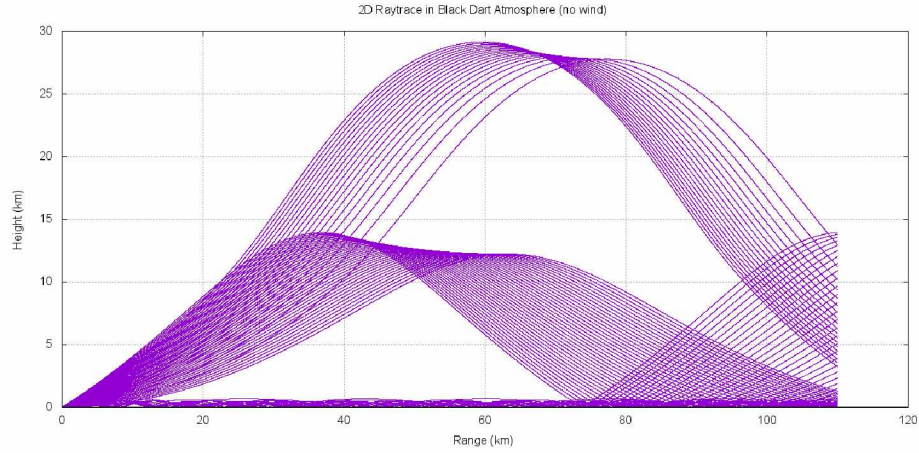


Figure 4.3: Ray trace through the Black Dart atmosphere.

Similar to the ray trace results using the canonical atmosphere, the ray trace results using the Black Dart atmosphere predict downward refracting rays at altitudes from 10–14 km. Investigation of the Black Dart atmospheric data (Figure 3.18) indicates the temperature profile should cause rays to refract towards the ground around an altitudes below 1 km and above 25 km. Figure 4.4 shows the effective sound speed, c_{eff} , as a function of temperature for the Black Dart atmospheric data.

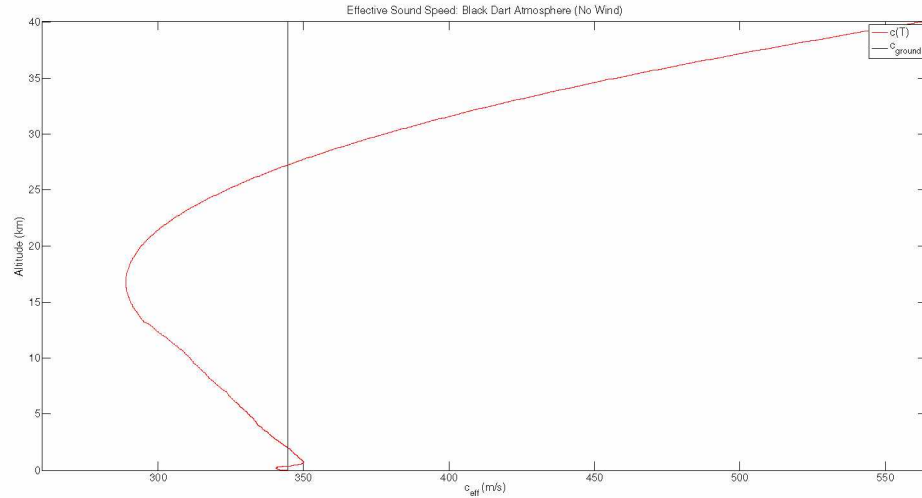


Figure 4.4: Effective sound speed of the Black Dart atmospheric data. Red is c_{eff} as a function of temperature. Black is the speed of sound at the ground.

The effective sound speed of the Black Dart atmosphere clearly indicates this should occur at an altitude below 1 km and above 25 km. It is currently unknown why the ray trace results using both the canonical atmosphere and Black Dart atmosphere predict downward refracting rays at altitudes between 10–14 km.

Figure 4.5 shows a more detailed view of the duct through the Black Dart atmosphere. This study focused on propagation ranges of 25, 60, and 100 km which seem to have strong arrival groupings.

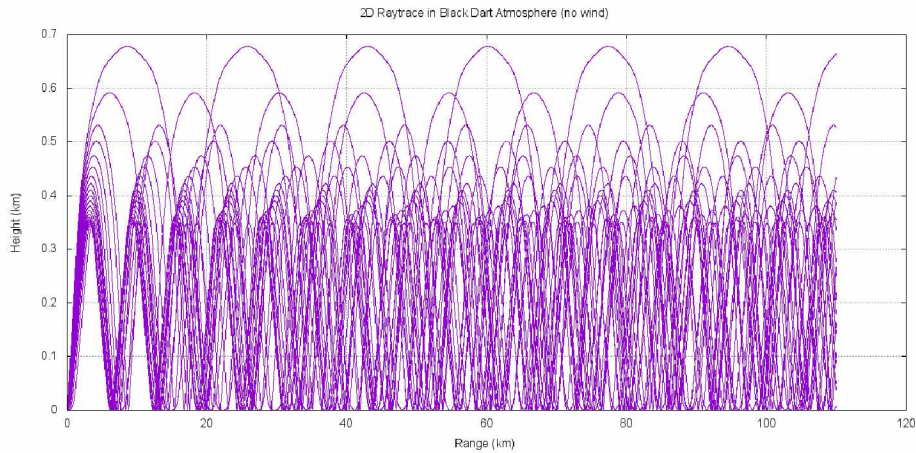


Figure 4.5: Ray trace through the Black Dart atmospheric duct.

The output of the NCPA ray trace subroutine includes estimates of the total travel time and maximum altitude reached for a given ray. These estimates provided the basis for choosing periods of 256 and 512 s for use in the ModBB subroutine.

4.2 ModBB

The NCPA ModBB subroutine was used to investigate propagation effects on a typical N-wave pulse, built into the code, for propagation ranges of 25, 60, and 100 km. The results of section 4.1.2 lead to selecting periods of 256 and 512 s. Figure 4.6 shows the source waveforms and their power spectra. These waveforms show power spectra grouped smoothly around their central maximum frequency.

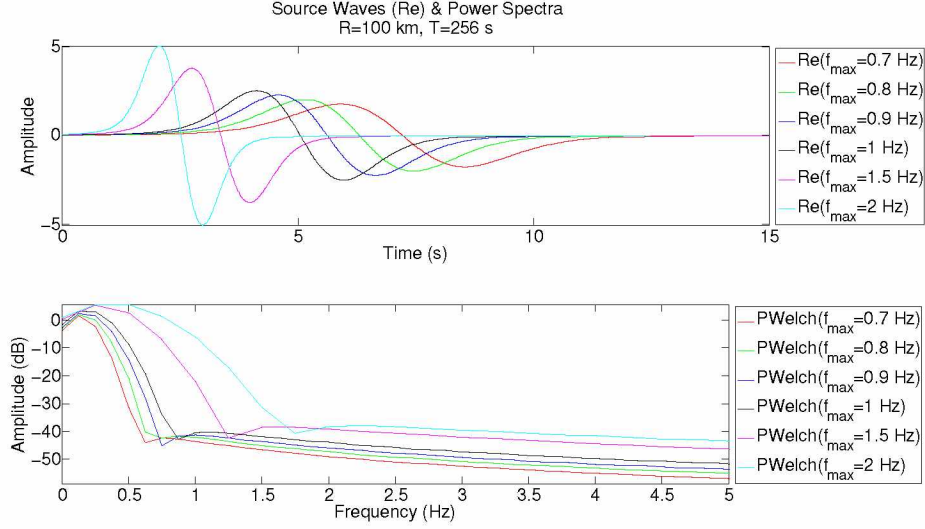


Figure 4.6: Initial source pulses used in the ModBB subroutine. Panel 1: the source waveforms. Panel 2: the power spectra of the initial waveforms.

The exact amplitude and frequency content of the source signal is unknown as there was no sensor on board the USS Dewey. However, other cannon signals have been reported to have a typical N-wave shape.^[2] While the source waveforms shown in Figure 4.6 are not likely to contain the correct frequency content nor have the same amplitude as the true source waveform from the USS Dewey's five inch cannon, they should still provide an acceptable approximation.

The built in impulsive waveforms are generated by the ModBB subroutine once given a maximum frequency and, optionally, a central maximum frequency. No modification to the central maximum frequency was made during this study and the default value of $f_{\max}/5$ was used for all initial waveforms. ModBB generates the initial waveforms based on work by Waxler et. al.^[15] During their study a pressure pulse was recorded at a distance of 1.7 km from an impulsive source. A Fourier transform was taken of this pulse and Eq. (4.1) was fitted to its spectrum.

$$Q(\omega) = A\omega e^{1/2(B\omega + (B\omega)^2)} \quad (4.1)$$

Once ModBB is given a maximum frequency it applies Eq. (4.1) to generate the source spectrum then uses an inverse Fourier transform to produce the initial waveforms shown in Figure 4.6.

During the course of this study it was determined that initial pulses with a maximum frequency larger than 2 Hz provided unreliable results. The ModBB subroutine was designed only for low frequency wave propagation. Despite the fact the true signal received at the infrasound array (JATO Row) contains frequency content up to 30–40 Hz, frequencies above

2 Hz were excluded from this study. The initial pulses used by the ModBB subroutine were slowly stepped up in maximum frequency content and are indicated by the “ f_{\max} ” value.

4.2.1 Canonical Atmosphere

A typical result of model propagation through the canonical atmosphere is shown in Figures 4.7 and 4.8. Panel 1 of the two figures show the model’s propagated waveforms vs time. Panel 2 of the two figures show the associated power spectra. Both figures show results for model propagation to a range of 100 km. A period of 256 s was used to generate the results of Figure 4.7 and a period of 512 s was used to generate the results of Figure 4.8. The amplitudes of the model’s propagated waves remain relatively similar as the maximum frequency content of the initial pulse used increases. This result will be shown to be different from results of model propagation through the Black Dart atmosphere.

The power spectra do show some frequencies contain more of the wave’s energy than others (indicated by the bumps). This is to be expected as some frequencies may attenuate less during propagation. The NCPA code accounts for this attenuation by employing Eq. (2.21). In general, the amplitude of the model’s propagated wave is greatly reduced when compared to the source waveforms. This effect could be due to the attenuation during propagation or the code failing to properly calculate the propagated waveforms.

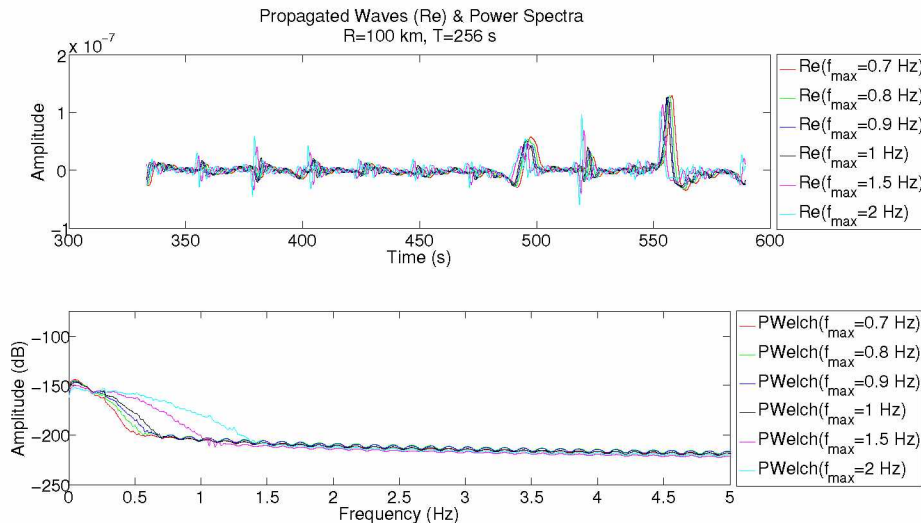


Figure 4.7: ModBB wave propagation to 100 km with a period of 256 s through the canonical atmosphere.

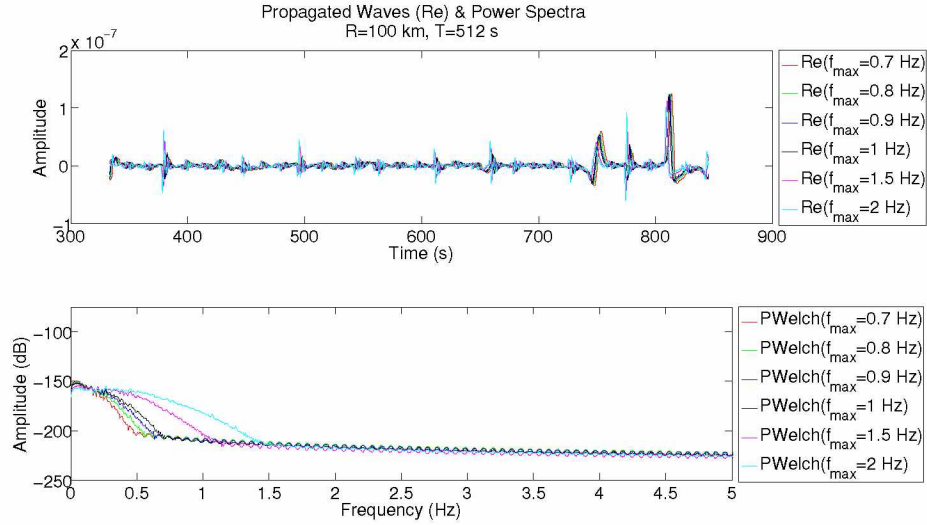


Figure 4.8: ModBB wave propagation to 100 km with a period of 512 s through the canonical atmosphere.

All of the propagation trials through the canonical atmosphere show strong arrivals near the end of the period, T . These results are therefore not self-consistent between the two periods used in this study. Further, the arrival times do not agree with the results of the ray trace subroutine. It is currently unknown what causes this discrepancy.

The lack of self-consistency between the two periods used and the extremely small amplitudes of the model's propagated waveforms generated by ModBB using the canonical atmosphere may indicate no viable signal. However, these trials and results are intended to be used as a comparative example for model propagation through an atmosphere without a strong lower temperature inversion. The results of trials using atmospheric data with a strong lower temperature inversion (see section 4.2.2) show similar model propagated wave amplitudes but are fundamentally different in their structure.

4.2.2 Black Dart Atmosphere

Figures 4.9 and 4.10 show the propagated waveforms and power spectra for propagation through the Black Dart atmosphere to a range of 25 km.

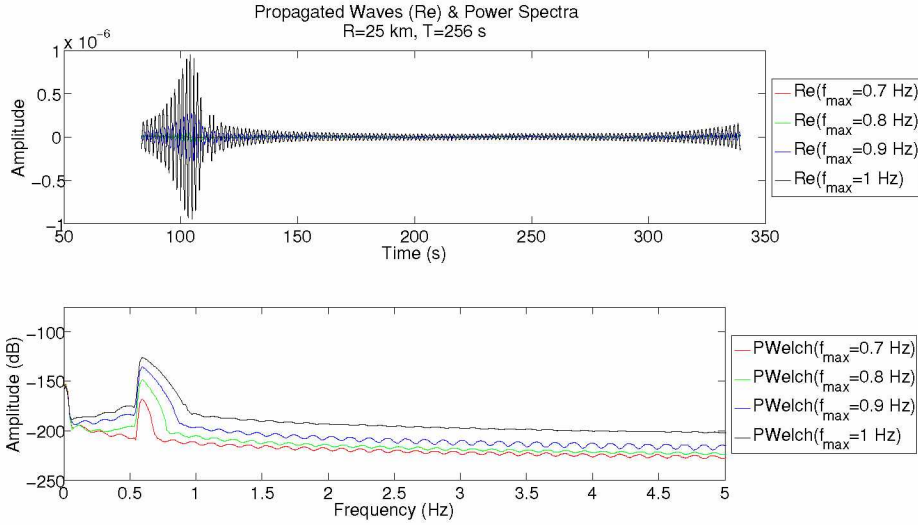


Figure 4.9: ModBB wave propagation to 25 km with a period of 256 s through the Black Dart atmosphere. Panel 1: the propagated waveforms. Panel 2: the power spectra of the propagated waveforms.

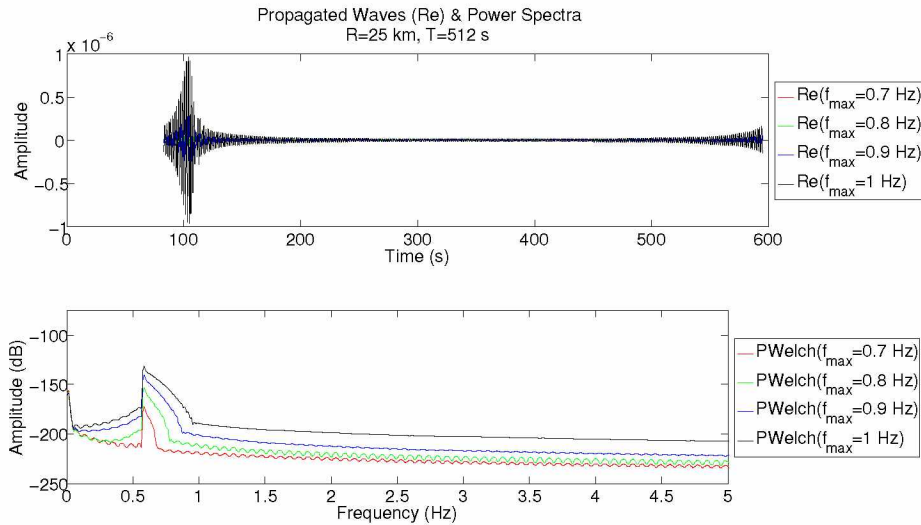


Figure 4.10: ModBB wave propagation to 25 km with a period of 512 s through the Black Dart atmosphere. Panel 1: the propagated waveforms. Panel 2: the power spectra of the propagated waveforms.

The amplitudes of the model's propagated waves increase with the maximum frequency content of the initial pulse used to generate them. That is to say, the amplitudes of the model's propagated waveforms is not self-consistent. This is most easily seen in panel 1 of Figure 4.9. The model propagated waveform resulting from propagation through the Black Dart atmosphere of an initial pulse with a maximum frequency of 1 Hz (black) is shown to have the largest amplitude. The propagated waveform for an initial pulse with a maximum frequency of 0.7 Hz (red) has an amplitude sufficiently small as to not be visible

when plotted against the other results. It is unclear if this is an accurate calculation or if the NCPA code is generating noisy or inaccurate results. The power spectra also show an increase in amplitude with higher maximum frequency content of the initial pulses. This lack of self-consistency in the model's propagated waveforms did not occur for propagation through the canonical atmosphere. It is worth noting, unlike the results of propagation through the canonical atmosphere, the time of arrival matches between the two time periods used for propagation through the Black Dart atmosphere.

The inconsistent amplitude of the model's propagated waveforms, oscillatory structure, and the self-consistency of the arrival times are typical results of all trials using the Black Dart atmosphere. Also, none of the results from the ModBB subroutine match the signal recorded at JATO Row (Figure 1.1).

Figures 4.11 and 4.12 show the propagated waveforms and power spectra for propagation to a range of 60 km through the Black Dart atmosphere.

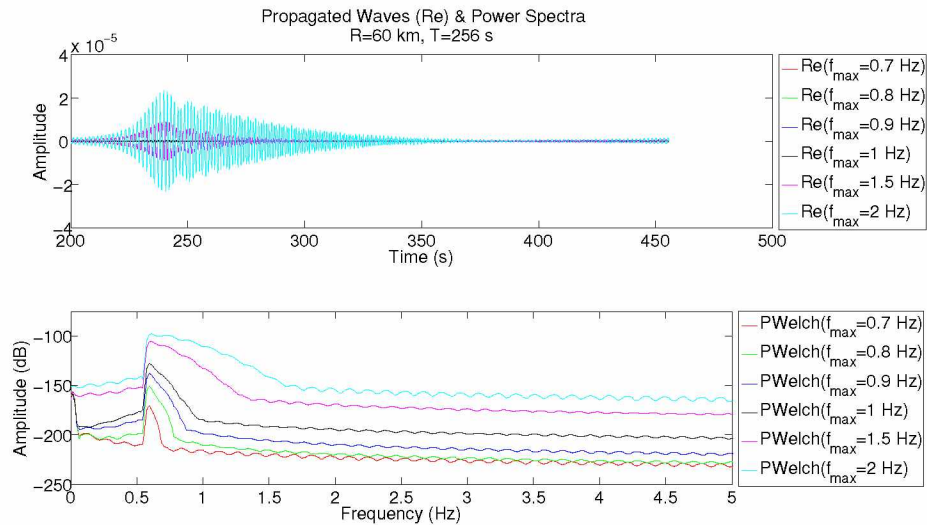


Figure 4.11: ModBB wave propagation to 60 km with a period of 256 s through the Black Dart atmosphere. Panel 1: the propagated waveforms. Panel 2: the power spectra of the propagated waveforms.

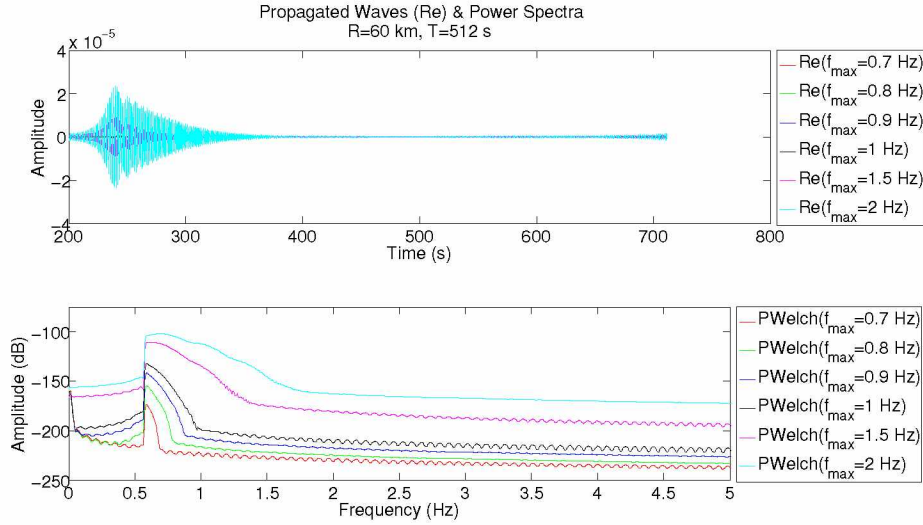


Figure 4.12: ModBB wave propagation to 60 km with a period of 512 s through the Black Dart atmosphere. Panel 1: the propagated waveforms. Panel 2: the power spectra of the propagated waveforms.

Propagation to 60 km shows a noticeable difference in the power spectra as the maximum frequency increases. The power spectra lose the smoothness seen in shorter propagation distance (Figures 4.9 and 4.10) and the source spectra (Figure 4.6). The bumps may be the result of attenuation effects or numerical errors in the NCPA code.

Similar to the results of propagation to 25 km, the model's propagated waveforms show strong oscillations. As the maximum frequency content of the initial pulse increases, the model's propagated waveform and its associated power spectra increase in amplitude. The model indicates the initial pulse with the lowest maximum frequency produces a propagated waveform with the smallest amplitude.

Figures 4.13 and 4.14 show the propagated waveforms and power spectra for propagation to a range of 100 km through the Black Dart atmosphere.

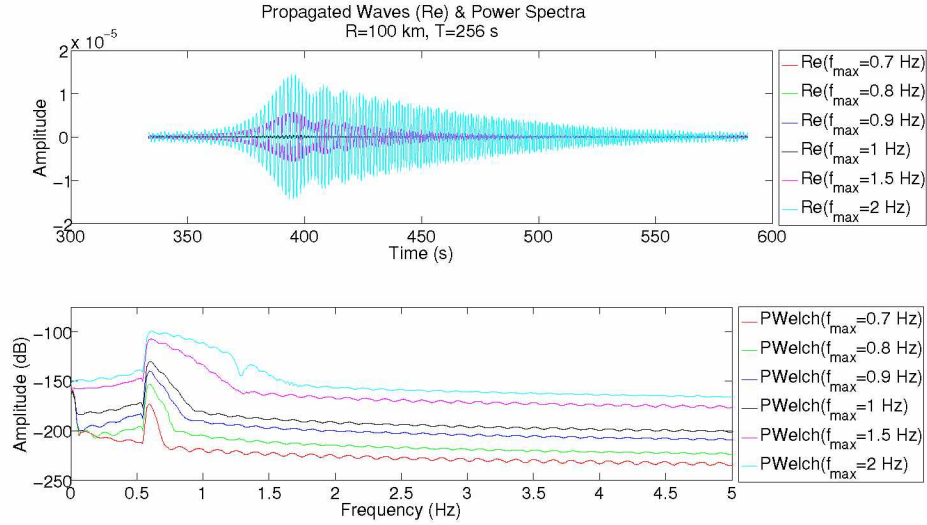


Figure 4.13: ModBB wave propagation to 100 km with a period of 256 s through the Black Dart atmosphere. Panel 1: the propagated waveforms. Panel 2: the power spectra of the propagated waveforms.

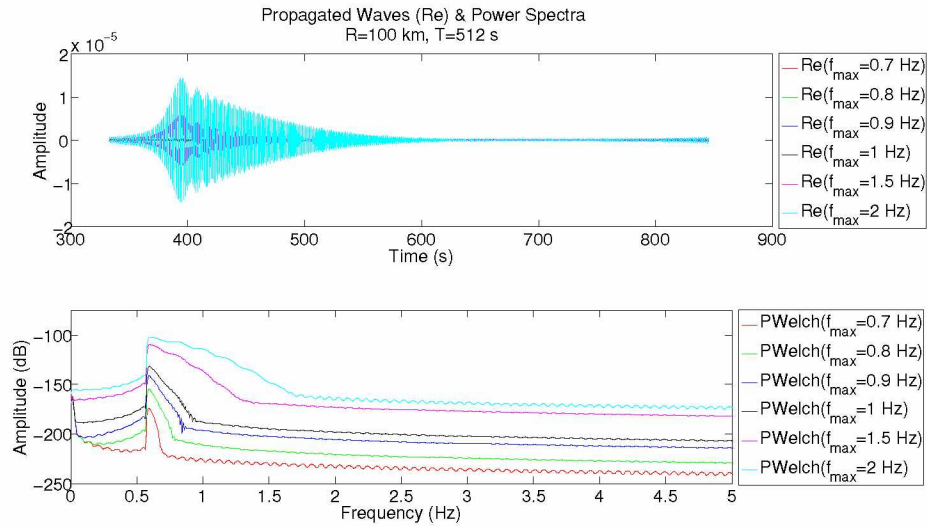


Figure 4.14: ModBB wave propagation to 100 km with a period of 512 s through the Black Dart atmosphere. Panel 1: the propagated waveforms. Panel 2: the power spectra of the propagated waveforms.

The power spectra for propagation to 100 km show more pronounced effects as those seen in the 60 km case. Small peaks are visible at various frequencies. This may be an indication some frequencies are ducted better than others or attenuated less and therefore contain more of the total wave energy. The frequencies with peaks in the power spectra are likely of the correct wavelength to show stronger arrivals than the frequencies with less power.

The major differences between the model's propagated waveforms through the canonical and Black Dart atmospheres are the timescale and structure of the propagated waves. The model waveforms resulting from propagation through the Black Dart atmosphere are much longer to the point of being unreliable. The true signal received on the infrasound array (JATO Row) had a duration of less than 5 s (see Figure 1.1). The model's propagated waveforms through the Black Dart atmosphere have durations on the order of 100 s. The model's waveforms propagated through the Black Dart atmosphere also show an oscillatory structure. This oscillatory structure did not occur in the model's propagated waveforms through the canonical atmosphere. The amplitude of the model's propagated waveforms was consistent for different initial pulses propagated through the canonical atmosphere but not for propagation through the Black Dart atmosphere.

One possible explanation for the characteristics of the Black Dart results may be the atmospheric profile. Specifically, the limited height. In order for the methodology of section 2.4 to function properly the atmosphere data needs to extend to high altitudes. This is the reason it was suggested to extend the atmosphere to a height of 40 km rather than leaving it at the 20 km as collected by the weather balloon.^[14] Further extension of the atmosphere to well beyond 100 km may improve the results presented here.

The arrival times agree between the 256 and 512 s trials for model propagation through the Black Dart Atmosphere and are in good agreement with those estimated by the NCPA ray trace subroutine. This lends support to the idea the pressure pulse from the source is being ducted by the lower atmospheric temperature inversion. However, the model's propagated waveforms are unreliable due to their long duration, small amplitude, and oscillatory structure. The ModBB subroutine does not produce any propagated waveforms similar to the signal received by the JATO Row sensor network (Figure 1.1) so the results of this study are inconclusive.

The spectrograms of the model's propagated waveforms are presented below. The spectrograms are plotted as frequency (Hz) vs. time (s) and the color bar indicates the power. For simplicity, only certain trials are shown which illustrate the general trends.

Panel 1 of Figure 4.15 shows the model's propagated waveform through the Black Dart atmosphere to a range of 25 km for an initial pulse with maximum frequency content of 0.9 Hz. Panel 2 shows its associated spectrogram. The arrival time of the model's propagated wave is roughly 100 s and the spectrogram shows an increase in frequency content with time. The increase is indicated by the higher power (red) peaks increasing in height from ~ 90 – 105 s which indicates higher frequency content in the wave arrives after lower frequency content. This may be an indication of dispersion occurring during

the simulated propagation through the Black Dart atmosphere by the ModBB subroutine. Increasing the propagation distance to 60 and 100 km yield similar results with the duration of the pulse arrival increased.

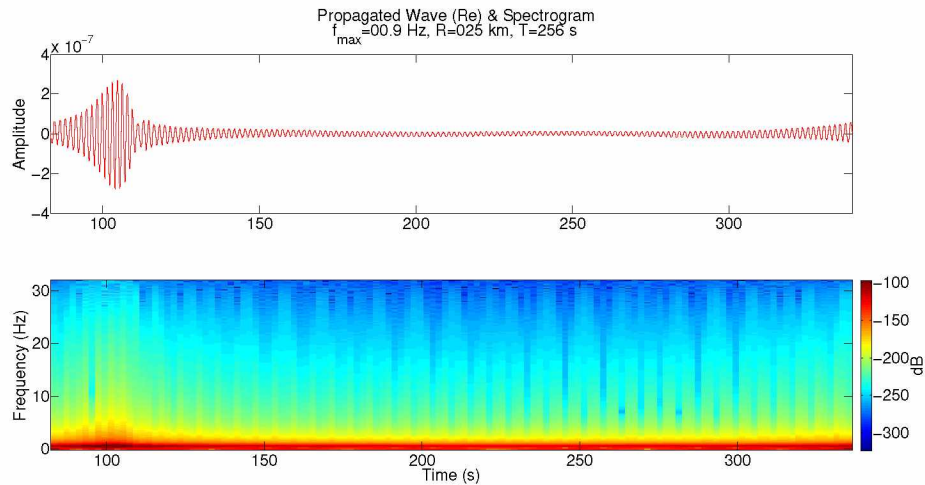


Figure 4.15: Propagated waveform through Black Dart Atmosphere and spectrogram to a range of 25 km with $f_{textmax} = 0.9$ Hz and $T=256$ s. Panel 1: propagated waveform through Black Dart atmosphere. Panel 2: spectrogram of the propagated waveform.

As the maximum frequency content of the initial pulse is increased to approximately ≥ 1.5 Hz a new structure is seen in the spectrogram of the model's propagated waveform. Panel 1 of Figure 4.16 shows the propagated waveform through the Black Dart atmosphere to a range of 60 km for an initial pulse with maximum frequency content of 2.0 Hz. Panel 2 shows its associated spectrogram. Similar to the lower maximum frequency content initial pulse propagated to a range of 25 km shown above, this higher maximum frequency content initial pulse propagated to a range of 60 km shows a ramp up, or dispersion, of the frequency content in the arriving waveform with time.

The first new feature visible is the multiple arriving packets. In this example there are three with a possible fourth appearing just after 350 s. It is unclear if these packets are a mathematical artifact, noise, or strong arrivals from different ray paths converging together.

The second new feature visible is a steady increase in power with frequency and time. The dark red in the spectrogram indicates the highest power content of the propagated wave shifts to higher frequencies as time increases. Additionally, another shift is visible beginning at approximately 360 s. This shift may indicate a high frequency tail. These results are more clearly visible as the period is increased.

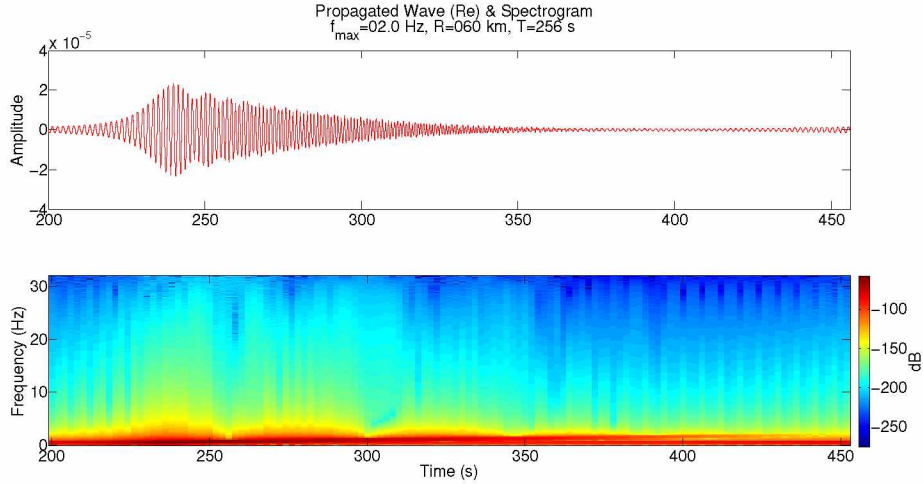


Figure 4.16: Propagated waveform through Black Dart Atmosphere and spectrogram to a range of 60 km with $f_{\text{textmax}} = 2.0$ Hz and T=256 s. Panel 1: propagated waveform through Black Dart atmosphere. Panel 2: spectrogram of the propagated waveform.

Panel 1 of Figure 4.17 shows the model’s propagated waveform through the Black Dart atmosphere to a range of 60 km for an initial pulse with maximum frequency content of 2.0 Hz and the period has been increased to T=512 s. Panel 2 shows its associated spectrogram. Similar to the T=256 s result shown above the multiple wave packets are visible and the highest power content (dark red) increases with frequency and time. The second shift is also now clearly visible and does not appear to be a numerical effect due to the window boundary. These results seem to indicate there is a high frequency tail in the model’s propagated waveforms which would lend evidence to dispersive atmospheric effects. However, the multiple “packets” are not consistent with the JATO Row signal (Figure 1.1).

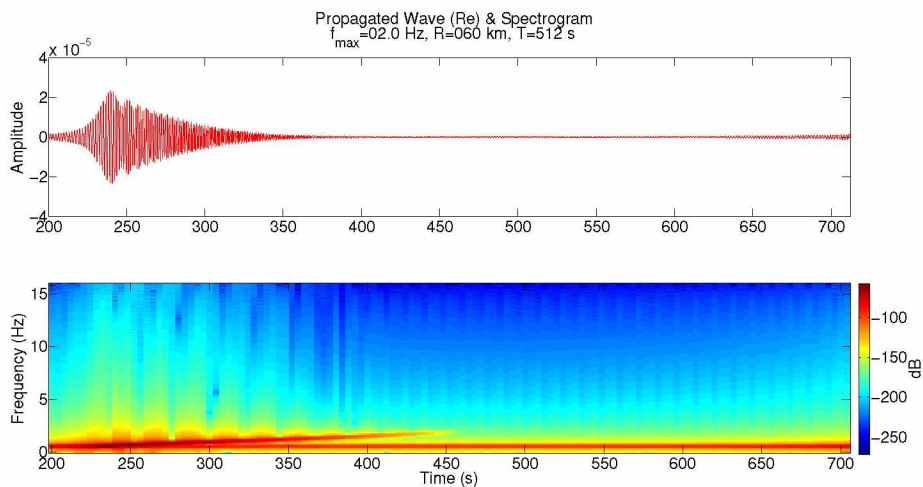


Figure 4.17: Propagated waveform through Black Dart Atmosphere and spectrogram to a range of 60 km with $f_{\text{textmax}} = 2.0$ Hz and T=512 s. Panel 1: propagated waveform through Black Dart atmosphere. Panel 2: spectrogram of the propagated waveform.

Investigation of the transmission loss vs. time for the model's propagated waveforms also indicates multiple arriving wave packets. Figure 4.18 shows the transmission loss vs. time for model propagation to a range of 25 km through the Black Dart atmosphere for an initial pulse with maximum frequency content of 0.9 Hz (Figure 4.15 shows the model's propagated waveform and spectrogram for this initial pulse).

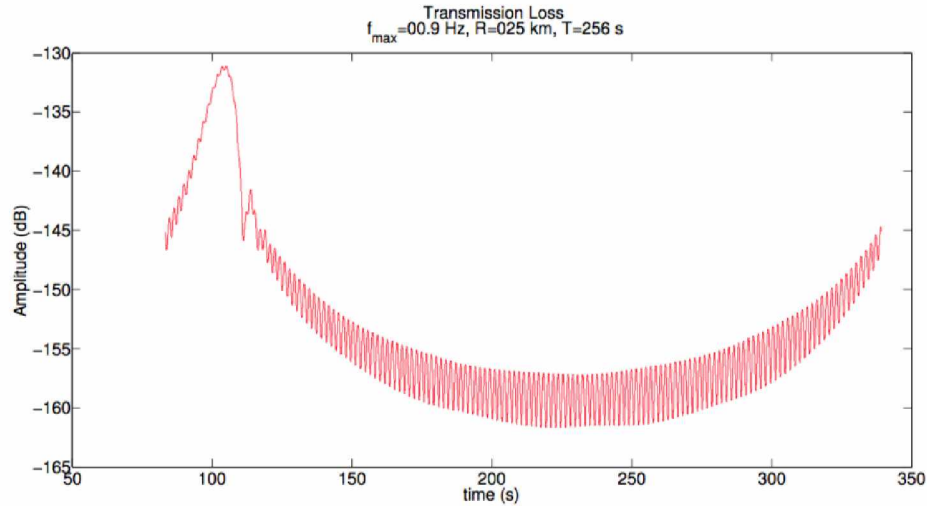


Figure 4.18: Transmission loss vs. time at a range of 25 km, $f_{\max}=0.9$ Hz and $T=256$ s.

Standard transmission loss figures are given as an amplitude (dB) vs. distance. However, the ModBB subroutine assumes a receiver exists at the specified propagation distance (25, 60, and 100 km were used in this study). Propagated solutions are generated for the duration of the specified time period (256 and 512 s were used in this study). The output of the ModBB subroutine contains time, real and imaginary components of the propagated wave pressure. The transmission loss (TL) is calculated in the usual way as $TL = 20 \times \log_{10} \left(\sqrt{\Re^2 + \Im^2} \right)$. The dB amplitude reference used in the ModBB subroutine is not specified in the help file (see Appendix A). However, the ray trace and parabolic equation subroutines use the pressure amplitude at a range of 1 km as the reference amplitude. It is assumed the ModBB subroutine does also and all dB values are in reference to the pressure amplitude at 1 km from the source.

Chapter 5 Conclusion

The results of the ModBB subroutine show a total disagreement when compared to the received signal (Figure 1.1). The discrepancies include the frequency content, duration, structure, and amplitude of the model's propagated waveforms.

The NCPA code was designed to model infrasonic propagation only. Results obtained from the use of initial pulses with a maximum frequency content above 2 Hz were unreliable and excluded from this study. The maximum frequency content of the received signal on the JATO Row sensors was approximately 40 Hz. The limitations on maximum frequency content in the initial pulses used with the ModBB subroutine severely impacted the NCPA code's ability to reproduce the signal recorded at JATO Row. Without an initial pulse which closely models the true source function of the USS Dewey's 5 inch deck gun and the NCPA code's unreliability in handling frequencies above 2 Hz, no viable model waveform could be generated.

The duration of the model's propagated waveforms from the ModBB subroutine are on the order of 10^2 s. The received signal had a duration on the order of 10^0 s. It is currently unknown why the model waveforms' durations are so much longer than the actual signal. However, comparison between the results using the canonical and Black Dart atmospheric data lend evidence to the limited atmospheric data gathered during the Black Dart exercises as a possible cause of the discrepancy. The NCPA code is built upon the mathematics of an eigenfunction expansion of the Helmholtz equation and uses a WKB approximation to patch the solutions with the boundary condition in the upper atmosphere (wave amplitudes should go to zero as the altitude approaches the upper edge of the atmosphere). The limited atmospheric data hinders the model's ability to solve for the proper eigenvalues and may be a cause of the waveform duration discrepancy. The limited atmospheric data may also be the cause of the oscillatory form of the model's propagated waveforms.

The amplitudes of the model's propagated waveforms from the ModBB subroutine are in an unspecified unit. The atmospheric pressure data is required to be in units of hectopascals (hPa) and other NCPA subroutines provide outputs in decibels (dB). The current working theory is that the propagated waveform amplitudes are in units of Pascals or hectopascals. With this assumption, the model's propagated amplitudes are all many orders of magnitude smaller than the received signals' amplitude. Also, the model amplitudes increase as the maximum frequency content of the initial pulse increases. Without ground truth as to the actual form of the source function it is unreasonable to assume any model's propagated waveform would match that of the received signal. As for the general increase in the amplitude of the model's propagated waveform with increasing maximum frequency content of the initial pulse used, it is currently unknown what causes this. One

possibility is that as higher frequency content is included more ducted modes occur in the lower temperature inversion waveguide. As more ducted modes are included more power of the initial wave will be contained within the duct and therefore reach the “receiver” located at the propagation distances of 25, 60, or 100 km. It is also likely the limited height of the atmospheric data is causing numerical errors in the ModBB subroutine which therefore generate unreliable propagated waveforms. These explanations are unconfirmed and the cause of the amplitude increase in the model’s propagated waveform as the maximum frequency content of the initial pulse increases is unknown.

Investigation of the model’s output waveforms from the ModBB subroutine show the code fails to produce a reliable signal, do to the structure, duration, and amplitude of the waveforms. Including a more complete atmospheric data file, such as from the Ground to Space (G2S) semi-empirical spectral model global atmospheric data, may allow the NCPA code to more accurately compute eigenvalues and eigenfunction solutions to the normal mode approximation of the Helmholtz equation. A sensor located at the source would allow a custom source function to be used with the ModBB subroutine which more accurately matches the true source signal. These two corrections are believed to be necessary for the NCPA code to provide a more accurate model of the propagated waveforms as recorded by the actual infrasound array (JATO Row).

The spectrograms of the model’s propagated waveforms generated by the ModBB subroutine do not match those of the actual received signals. However, both the model and the actual received signal show the initial arrival of the propagated wave contains low frequency content followed by a high frequency tail. This result is interesting due to it being contradictory to standard dispersion relations (see Figure 2.1). Dispersion relations given for the canonical wave equation^[3] and Helmholtz equation^[15] show the lower frequency content of a wave should travel slower than the higher frequency content, thus resulting in a low frequency tail. It is possible the low frequency content of the source wave is not ducted well by the lower temperature inversion waveguide. The low frequency content of the received signal may instead be a direct line-of-sight arrival from the source to the receiver. The higher frequency content of the source wave may actually be ducted by the waveguide but due to the longer ray path would arrive after the direct line-of-sight arrival. These two different ray paths might account for the high frequency tail recorded by the infrasound sensors and predicted by the NCPA model. However, this explanation is unconfirmed. The true source of the observed high frequency tail is unknown.

A summary of the results and conclusions drawn from this study are listed below:

- The NCPA ray trace subroutine indicates the strong temperature inversion in the lower atmosphere creates a ducting waveguide at ≈ 0.5 km.

- The NCPA ModBB subroutine fails to model the signal recorded at JATO Row:
 - The amplitude of the model's propagated waveforms are small by comparison to received signal.
 - The model's propagated waveforms show an oscillatory structure not seen in the received signal.
 - The duration of the model's propagated waveforms is of the wrong order of magnitude.
- The spectrograms of the model's propagated waveforms do indicate a high frequency tail as seen in the received signal.

References

- [1] Arnoult, K. M., Olson, J. V., Szuberla, C. A. L., McNutt, S. R., Garcés, M. A., Fee, D., and Hedlin, M. A. H. (2010). Infrasound observations of the 2008 explosive eruptions of Okmok and Kasatochi volcanoes, Alaska. *Journal of Geophysical Research: Atmospheres*, 115(D2).
- [2] Baker, W. E. (1973). *Explosions in Air*. University of Texas Press.
- [3] Bristow, W. A., Greenwald, R. A., and Villain, J. P. (1996). On the seasonal dependence of medium-scale atmospheric gravity waves in the upper atmosphere at high latitudes. *Journal of Geophysical Research: Space Physics*, 101(A7):15685–15699.
- [4] CTBTO Preparatory Commission (2015). Station profiles. <https://www.ctbto.org/verification-regime/station-profiles>.
- [5] Jensen, F. B., Kuperman, W. A., Porter, M. B., and Schmidt, H. (1994). *Computational Ocean Acoustics*. American Institute of Physics.
- [6] Negraru, P. T. and Herrin, E. T. (2009). On infrasound waveguides and dispersion. *Seismological Research Letters*, 80(4):565–571.
- [7] Olson, J. V. and Szuberla, C. A. L. (2005). Distribution of wave packet sizes in microbarom wave trains observed in alaska. *Journal of the Acoustical Society of America*, 117(3):1032.
- [8] Reijo Rasinkangas (2008). Dispersion relation. <https://wiki oulu.fi/display/SpaceWiki/Dispersion+relation>. Accessed: 2015-11-01.
- [9] Salomons, E. M. (2001). *Computational Atmospheric Acoustics*. Kluwer Academic Publishers.
- [10] Skowbo, E. (2012). Infrasound mobile MASINT unattended ground sensor (M2UGS) system: Introduction and Black Dart “quick look” results. Lecture Presentation.
- [11] Skowbo, E. (2015). Personal Communication.
- [12] Waxler, R. (2002). A vertical eigenfunction expansion for the proagation of sound in a downward refracting atmosphere over a complex impedance plane. *Acoustical Society of America*, 112(6):2540–2552.
- [13] Waxler, R. (2004). Modal expansions for sound propagation in the nocturnal boundary layer. *Acoustical Society of America*, 115(4):1437–1448.
- [14] Waxler, R. (2014). Personal Communication.

- [15] Waxler, R., Gilbert, K. E., and Talmadge, C. (2008). A theoretical treatment of the long range propagation of impulsive signals under strongly ducted nocturnal conditions. *Acoustical Society of America*, 124(5):2742–2754.
- [16] Waxler, R., Talmidge, C. L., Dravida, S., and Gilbert, K. E. (2006). The near-ground structure of the nocturnal sound field. *Acoustical Society of America*, 119(1):86–95.

Appendix A ModBB Help File

The following pages contain the help file for the NCPA ModBB subroutine as they appear in the NCPA code distribution as of 28 August 2015.

1 ModBB - Pulse (broad-band) propagation based on Normal Modes

ModBB propagates an infrasound pulse (or waveform) in a range-independent stratified atmosphere. The propagation can be performed with either ModESS or WMod single-frequency algorithms. The attenuation in the air is taken into account as a perturbation. A pulse with given bandwidth and center frequency is propagated to a specified distance.

1.1 Mathematical Problem

If option `--use_modess` is chosen **ModBB** solves the following Helmholtz equation in 2 dimensions for a point source in a stratified atmosphere with horizontal wind and over rigid ground (see also **ModESS**):

$$\left[\frac{1}{r} \frac{\partial}{\partial r} \left(r \frac{\partial}{\partial r} \right) + \rho_0(z) \frac{\partial}{\partial z} \left(\frac{1}{\rho_0(z)} \frac{\partial}{\partial z} \right) + \frac{\omega^2}{c_{eff}^2(z)} \right] p(r, z) = -\frac{\delta(r)\delta(z - z_s)}{2\pi r}$$

where $p(r, z)$ is the pressure at range r and height z , ω is the angular frequency, $\rho_0(z)$ is the air density and $c_{eff}(z)$ is the effective (complex) sound speed i.e. the sum of the sound speed and the wind velocity component in the (horizontal) direction of wave propagation, $\hat{\mathbf{k}}_r$:

$$c_{eff}(z) = c(z) + \mathbf{v}_0(z) \cdot \hat{\mathbf{k}}_r + ia(\omega)$$

The ia term accounts for atmospheric absorption and damping of the acoustic energy. ModESS is based on the Effective Sound Speed Approximation which is valid for near-horizontal propagation angles and relatively low wind speeds (low Mach numbers).

If option `--use_wmod` is chosen **ModBB** solves the following Helmholtz equation (see also **WMod**):

$$\left[\frac{1}{r} \frac{\partial}{\partial r} \left(r \frac{\partial}{\partial r} \right) + \rho_0(z) \frac{\partial}{\partial z} \left(\frac{1}{\rho_0(z)} \frac{\partial}{\partial z} \right) + \frac{(\omega + i\mathbf{v}_0 \cdot \nabla_r)^2}{c^2(z)} \right] p(r, z) = -\frac{\delta(r)\delta(z - z_s)}{2\pi r}$$

where $p(r, z)$ is the pressure at horizontal position \mathbf{x}_H and height z , ω is the angular frequency, $\rho_0(z)$ is the air density, $\mathbf{v}_0(z)$ is the horizontal wind speed and $\nabla_r = \frac{\partial}{\partial r} \mathbf{e}_r$ is the radial part of the gradient operator. The sound speed, $c(z)$, can be complex with the imaginary part accounting for atmospheric absorption and damping of the acoustic energy.

The boundary conditions are:

$$\begin{aligned} \frac{\partial p}{\partial z} \Big|_{z=0} &= 0 \\ p(r, z_{max}) &= 0 \end{aligned}$$

where z_{max} is the maximum altitude typically greater than 150 km.

The solution is obtained by the method of normal modes (see e.g. F. B. Jensen, W. A. Kuperman, M.B. Porter, H. Schmidt, "Computational Ocean Acoustics"; Chapter 5, AIP Press, 1994.).

1.2 Running ModBB (quick start)

Let's propagate a pulse from the source to a specified receiver. Two steps must be completed:

1. A dispersion file must be available or computed by using option `--out_disp_src2rcv_file`
2. Perform pulse propagation from source to receiver at one specified range (option `--pulse_prop_src2rcv`).

Obtaining the dispersion file

In Step 1 we compute the dispersion file. For example:

```
../bin/ModBB --out_disp_src2rcv_file myDispersionFile.dat
              --atmosfile NCPA_canonical_profile_zuvwtdp.dat
              --atmosfileorder zuvwtdp --azimuth 90
              --f_min 0.001953125 --f_step 0.001953125 --f_max 0.5
              --use_modess
```

This example is for the default *ground-to-ground propagation* in the direction of 90 degrees azimuth (from North) for a pulse of bandwidth specified by `--f_min`, `--f_step`, `--f_max`. Note that we request to `use_modess` algorithm. The output (dispersion) file is `myDispersionFile.dat`. Each line in this dispersion file has the format:

$freq, N_m, \rho(z_{src}), \rho(z_{rcv}), \text{Re}(k_m), \text{Im}(k_m), \Psi_m(z_{src}), \Psi_m(z_{rcv})$

where the index m varies from 1 to the number of modes N_m at the particular frequency $freq$.

By default the propagation is done up to 1000 km in range. For propagation other than ground-to-ground the user must specify the source height, `--sourceheight_km` and/or the receiver height `--receiverheight_km` (both referenced above ground level - AGL). The atmospheric profiles are specified in a column-based text file `NCPA\canonical\profile\zuvwtdp.dat`. The columns order is specified with option `--atmosfileorder`. In the above example the profile file has 7 columns in the following order `zuvwtdp`. Note that the physical units are NOT all in SI:

```
z - altitude [ km above Mean Sea Level (MSL) ]
u - West-to-East wind speed [ m/s ]
v - South-to-North wind speed [ m/s ]
w - vertical wind (usually zero) [ m/s ]
t - temperature [ Kelvin ]
d - density [ g/cm^3 ] !! not kg/m^3
p - ambient pressure [ hectoPascals ] !! not Pa
```

Pulse propagation example

We can now propagate a pulse to a point on the ground at `range_R_km`. As initial (source) pulse we can ask to use the provided built-in pulse with option `--use_builtin_pulse`. An example of an initial pulse is shown in Figure 1 corresponding to the frequency band found in the dispersion file from the previous example. The output is saved in file `mywavf.dat` and is plotted in Figure 2.

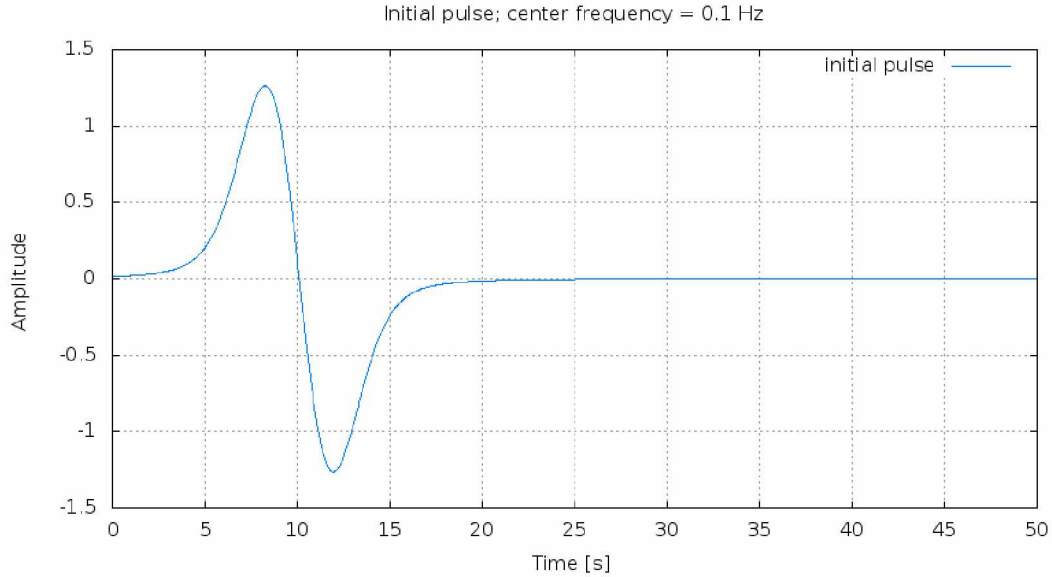


Figure 1: The built-in initial pulse: its spectrum has a center frequency of 0.1 Hz and maximum frequency of 0.5 Hz.

```
../bin/ModBB --pulse_prop_src2rcv myDispersionFile.dat --range_R_km 240
              --waveform_out_file mywavf.dat --use_builtin_pulse
```

Source type options

There are a total of 4 source types the user can employ. In addition to `--use_builtin_pulse` the user can:

- request the impulse response i.e a delta function as source; option `--get_impulse_resp`
- provide the source spectrum in a file; option `--src_spectrum_file`
- provide the source pulse (waveform) in a file; option `--src_waveform_file`

The user is responsible to provide waveforms or source spectra that are band limited within the frequency band of the dispersion file being used.

Computing the 2D pressure field

In this case the receivers are not just on the ground but on a 2D grid. The dispersion information is stored in binary files: one file per frequency. The name of the file has the format `<stub><frequency>_nm.bin` where the stub name is provided by user. In the example below the stub name is `disp2d`. Thus we compute 256 dispersion files for propagation to all receivers on a 2D grid for 256 frequencies from 0 to 0.5 Hz in steps of $0.5/256$ Hz:

```
../bin/ModBB --out_dispersion_files disp2d
```

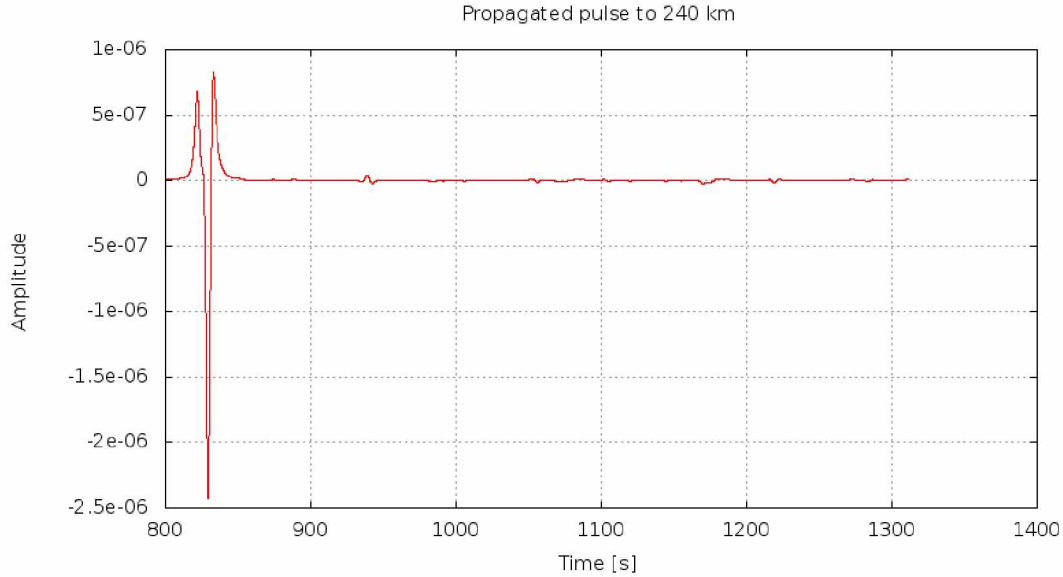



Figure 2: Propagated pulse to 240 km vs time. The default celerity of 300 m/s was used; hence the time window starts at the reduced time of 800 seconds.

```
--atmosfile NCPA_canonical_profile_zuvwtdp.dat
--atmosfileorder zuvwtdp --skiplines 0 --azimuth 90
--f_step 0.001953125 --f_max 0.5 --use_modess
```

At the end of the computation it is recommended to move all dispersion files to a directory e.g. `myDispersionFolder`. The next step is to use option `--pulse_prop_grid` to obtain pressure field spatial snapshots (frames) in a 2D "window". For example:

```
../bin/ModBB --pulse_prop_grid myDispersionFolder --R_start_km 220
--width_km 50 --height_km 25 --max_celerity 300 --tmstep 30
--ntsteps 5 --frame_file_stub myPressure --use_builtin_pulse
```

Note that this operation is computationally intensive as the pressure field is computed at all points on a 50 km x 25 km 2D x-z grid. Option `R_start_km 220` specifies that the grid is to start at 220 km from source; it will span from 220 km to 270 km in range and will be 25 km in height. The vertical resolution is given by the ratio of the maximum height to the number of points on the z-grid: $\Delta z = \text{maxheight_km} / \text{Nz_grid}$. By default the maximum height is 150 km and the default `Nz_grid=20000`; the horizontal spatial resolution is the same as in the vertical direction i.e. $\Delta x = \Delta z$.

In the above example we requested a total of 5 snapshots with option `--ntsteps=5` standing for "number of time steps". The time interval between these snapshots is 30 seconds as specified by `--tmstep 30`. Each of the five 2D field snapshots (frames) is saved in a binary file with the name `<frame_file_stub><reduced_time>.bin` as specified in option `-frame_file_stub myPressure`.

The reduced time for the first frame is determined from $R_start_km/max_celerity$ in seconds; the second frame will be a snapshot of the propagation 30 seconds later and so on. The binary snapshots (frame) files have the following format: the grid points N_z , N_x followed by the grid spacing, Δz , $R_start_km*1000$ [meters] and the reduced time. The N_x by N_z 2D field is stored next. The following pseudo-code snippet (Matlab) can be used to visualize the 2D field. An example is given in Figure 3.

```

fn    = 'myPressure_823.bin'      % name of file storing the field snapshot
fid   = fopen(fullfile(dirn, fn), 'r')
Nz    = fread(fid, 1, 'int')
Nx    = fread(fid, 1, 'int')
delZ  = fread(fid, 1, 'double') % grid resolution
r1    = fread(fid, 1, 'double') % this is R_start_km*1000 [meters]
tt    = fread(fid, 1, 'double') % reduced time i.e. 823 seconds in this case

% load 2D field in matrix M
M = zeros(Nz,Nx);
for i=1:Nz
    for j=1:Nx
        M(i,j) = fread(fid, 1, 'double');
    end
end

fclose(fid);

%%
x_km = (r1 + (0:(Nx-1))*delZ)/1000;
y_km = (0:(Nz-1))*delZ/1000;

%% plot 2D field
figure
imagesc(x_km,y_km,M)
axis xy
hold on
colorbar
xlabel('Range [km]')
ylabel('Height [km]')
title('2D pressure')

```

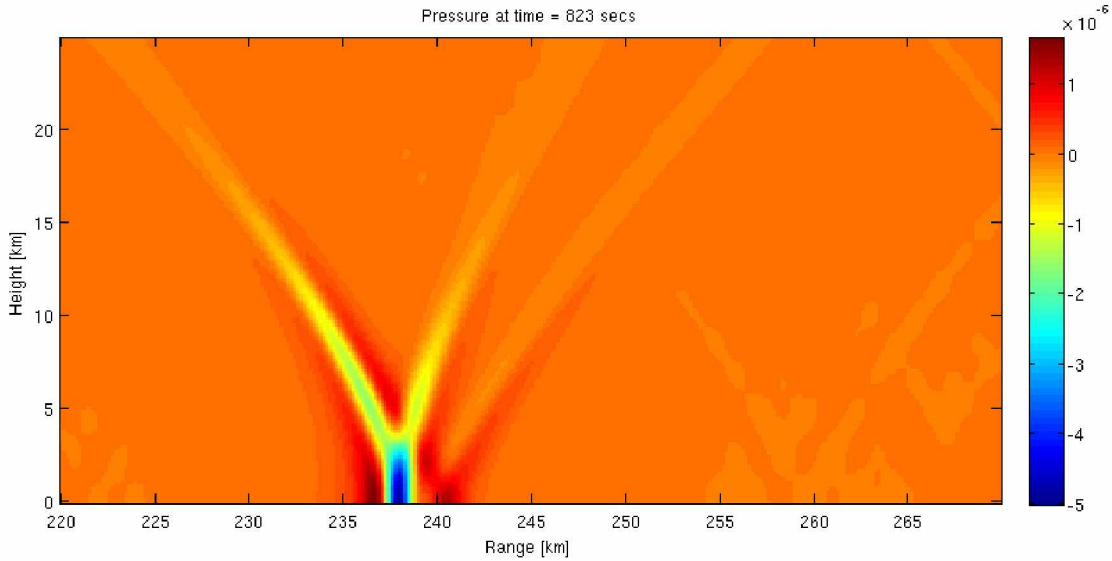


Figure 3: Example of 2D field.

1.3 Running ModBB (detailed)

```

-----
|                               NCPA Infrasound                               |
|                               Normal Modes Broadband                       |
|   Based on either: Effective Sound Speed Approximation - see ModESS       |
|                               Wide_Angle High-Mach code - see WMod         |
|                                                                           |
-----

```

Usage:

The options below can be specified in a colon-separated file "ModBB.options" or at the command line. Command-line options override file options.

```
--help -h          Print this message and exit
```

One of two algorithms can be used to perform pulse propagation. The first is based on the Effective Sound Speed Approximation (as in ModESS); the second is based on the the Wide_Angle High-Mach solution of the wave equation (see implementation in WMod).

ModESS is faster but it is accurate for (launch) angles less than 30 deg and low wind speeds. WMod extends the validity to higher angles and high Mach numbers but it runs slower.

Options `--use_modess` and `--use_wmod` allow the user to choose the desired algorithm when computing the dispersion data (see step 1 below).

To propagate a pulse, 2 steps must be completed:

1. A dispersion file must be available or computed

use either option `--out_dispersion_files` or `--out_disp_src2rcv_file`

2. Perform pulse propagation for one of several scenarios:
 - a. source-to-receiver at one range (option `--pulse_prop_src2rcv`)
 - b. source-to-receiver at several equally spaced ranges (option `--pulse_prop_src2rcv_grid`)
 - c. computing the whole 2D pressure field (most expensive - option `--pulse_prop_grid`)

For propagation the source type can be:

delta function -> see option `--get_impulse_resp`
built-in pulse -> see option `--use_builtin_pulse`
user-provided spectrum file -> see option `--src_spectrum_file`
user-provided waveform file -> see option `--src_waveform_file`

To compute a dispersion file one of the following 2 options is REQUIRED:

`--out_disp_src2rcv_file` <dispersion filename>
Output dispersion curves and modal values for source-to-receiver propagation to the specified file

`--out_dispersion_files` <dispersion filename stub>
Output dispersion curves and modal values on a 2D grid to binary files at each frequency. The resulting filenames have the stub and frequency appended:
e.g. <stub><freq>_nm.bin.
This option is computationally expensive.

Examples (run in the 'samples' directory):

- a. Compute dispersion file that will be used to compute the pressure pulse at 1 receiver. Assume that we want to end up with a pulse having a spectrum with a maximum frequency of $f_{\max}=0.5$ Hz. Also assume that we want the pulse represented on a time record of $T=512$ seconds. The number of positive frequencies necessary for the calculation is $T*f_{\max} = 256$ i.e. 256 frequencies between 0 and 0.5 Hz. Thus we know $f_{\max}=0.5$ Hz and $f_{\text{step}}=f_{\max}/256=0.001953125$ Hz. The corresponding run command is:

```
../bin/ModBB --out_disp_src2rcv_file myDispersionFile.dat
--atmosfile NCPA_canonical_profile_zuvwtdp.dat
--atmosfileorder zuvwtdp --skiplines 0 --azimuth 90
--f_step 0.001953125 --f_max 0.5 --use_modess
```

Each line in this dispersion file has the format:

freq n_modes rho_src rho_rcv Re(k_pert) Im(k_pert) V_m(z_src) V_m(z_rcv)
where m varies from 1 to n_modes.

- b. Compute dispersion files for propagation to all receivers on a 2D grid: for 256 frequencies from 0 to 0.5 Hz in steps of 0.5/256 Hz:

```

../bin/ModBB --out_dispersion_files disprs
              --atmosfile NCPA_canonical_profile_zuvwtdp.dat
              --atmosfileorder zuvwtdp --skiplines 0 --azimuth 90
              --f_step 0.001953125 --f_max 0.5 --use_modess

```

In addition the following options are REQUIRED:

```

--use_modess      Prompts the use of ModESS algorithm.
--use_wmod        Prompts the use of WMod algorithm.
Note that --use_modess and --use_wmod are mutually exclusive.
--atmosfile <filename>  Uses an ASCII atmosphere file
                        referenced to Mean Sea Level (MSL).
--atmosfileorder  The order of the (z,t,u,v,w,p,d) fields in
                        the ASCII file (Ex: 'ztuvpd')
--skiplines       Lines at the beginning of the ASCII file to skip
--azimuth         Value in range [0,360), clockwise from North
--f_step          The frequency step
--f_max           Maximum frequency to propagate
    Note that in this case the array of frequencies is [f_step:f_step:f_max].

```

OPTIONAL [defaults]:

```

--f_min           Minimum frequency [f_step Hz]
--maxheight_km   Calculation grid height in km above MSL [150 km]
--zground_km     Height of the ground level above MSL [0 km]
--Nz_grid        Number of points on the z-grid from ground to maxheight
                [20000]
--sourceheight_km Source height in km Above Ground Level (AGL) [0]
--receiverheight_km Receiver height in km AGL [0]
--maxrange_km    Maximum horizontal distance from origin to propagate
                [1000 km]
--ground_impedance_model Name of the ground impedance models to be employed:
                [rigid], TBD
--Lamb_wave_BC   For a rigid ground: if ==1 it sets
                admittance= -1/2*dln(rho)/dz; [ 0 ]
--wind_units     Use it to specify 'kmpersec' if the winds are given
                in km/s [mpersec]

```

Options for PULSE PROPAGATION:

```

--pulse_prop_src2rcv <dispersion filename>
                    Propagate pulse from source to 1 receiver
                    at a distance specified by option --range_R_km;
--range_R_km        Propagate pulse to this range [km]
--waveform_out_file <waveform filename>  Name of the waveform output file

--pulse_prop_src2rcv_grid <dispersion filename>
                    Propagate pulse from source to array of

```

horizontally equally-spaced receivers

REQUIRED additional options:

--R_start_km Propagation from this range to R_end_km in DR_km steps.
--R_end_km Pulse is propagated from R_start_km to this range.
--DR_km Range step to propagate from R_start_km to R_end_km.
--waveform_out_file <waveform filename>
 Name of the waveform output file.

OPTIONAL [defaults]:

--f_center The center frequency of the pulse; must be $\leq [f_{\max}/5]$.
--max_celerity Maximum celerity [300 m/s].

SOURCE TYPE options: Use one of the following 4 options to specify the source:

--get_impulse_resp Flag to use a delta function as source and
 to output the impulse response.
--use_built_in_pulse Flag to request the use of the built-in source pulse.
--src_spectrum_file Specify the file name of the source spectrum
 at positive frequencies. The file must have 3 columns
 | Freq | Real(Spectrum) | Imag(Spectrum) |
--src_waveform_file Specify the file name of the user-provided
 source waveform. The file must have 2 columns
 | Time | Amplitude |

If none of the source type options are specified the delta function source is the default i.e. the output is the impulse response.

Example: Pulse propagation to a point on the ground at range_R_km
and output the impulse response:

```
../bin/ModBB --pulse_prop_src2rcv myDispersionFile.dat --range_R_km 240  
            --waveform_out_file mywavf.dat --get_impulse_resp
```

Example: Pulse propagation to a point on the ground at range_R_km
and employ the user-provided source spectrum:

```
../bin/ModBB --pulse_prop_src2rcv myDispersionFile.dat --range_R_km 240  
            --waveform_out_file mywavf.dat --max_celerity 300  
            --src_spectrum_file source_spectrum_example.dat
```

Example: Pulse propagation to several points on the ground 20 km apart
and employ the user-provided source waveform:

```
../bin/ModBB --pulse_prop_src2rcv_grid myDispersionFile.dat  
            --R_start_km 240 --DR_km 20 --R_end_km 300  
            --waveform_out_file mywavf.dat
```

```
--src_waveform_file source_waveform_input_example.dat
```

To compute 2D field:

```
--pulse_prop_grid <dispersion directory name>
    Compute/view pulse on the 2D spatial x-z grid of 'height_km'
    and 'width_km' starting at 'R_start_km'
```

```
-----
height_km  |
            | Pressure field computed within |
            | a 2D (width_km x height_km) grid |
            |           'ntsteps' times       |
            |           every 'tmstep' seconds |
            |                                 |
            |                                 |
            |                                 |
-----x-----
            |
            | R_start_km
```

Additional parameters:

```
--R_start_km    The grid (viewing window) starts at R_start_km
--width_km      Grid width
--max_celerity  Reference speed [m/s]; in conjunction with R_start_km
                it is determining where inside the grid the field is at
                a time step; a value smaller than the speed of sound
                at the ground is suggested.
--tmstep        2D pressure field is calculated at this specified time step.
--ntsteps       Number of times the 2D pressure field is calculated
                'tmstep' seconds apart.
```

OPTIONAL [defaults]:

```
--height_km    The height of the 2D grid. [maximum height]
--frame_file_stub Each 2D grid is saved into a file with the name
                frame_file_stub_<time_of_start>; Default:[Pressure2D].
```

Example:

```
../bin/ModBB --pulse_prop_grid mydispersionFolder --R_start_km 220
              --width_km 50 --height_km 25 --max_celerity 300 --tmstep 30
              --ntsteps 5 --frame_file_stub myPressure --use_builtin_pulse
```